ELSEVIER

Palaeogeography, Palaeoclimatology, Palaeoecology 117 (1995) 153–184

PALAEO GEOGRAPHY CLIMATOLOGY ECOLOGY

Palaeoenvironments of the dinosaur-bearing Lameta Beds (Maastrichtian), Narmada Valley, Central India

S.K. Tandon, [a] A. Sood, [a] J.E. Andrews [b], P.F. Dennis [b]

[a] *Department of Geology, University of Delhi, Delhi-110007, India*
[b] *School of Environmental Sciences, University of East Anglia, Norwich, NR4 7TJ, UK*

Received 7 June 1994; revised and accepted 14 November 1994

Abstract

The Maastrichtian Lameta Beds of central India are intimately associated with the Deccan lavas and are critical to determining Upper Cretaceous palaeoenvironments and palaeogeography of the area. In the type Jabalpur sub-region, four mappable units of the Lameta Beds are recognised. The basal Green Sandstone is interpreted as a braided stream deposit. The Lower Limestone, characterised by brecciation and shrinkage cracks, is interpreted as a sub-aerially exposed palustrine flat with calcrete formation occurring on topographic highs of low relief plains. The overlying Mottled Nodular Beds exhibit a variable range of calcrete fabrics and morphologies including circum-granular and linear cracks, root casts and nodules. These are interpreted as pedogenically modified sheet wash deposits of a semi-arid alluvial plain. The Upper Sandstone is a sheet flood deposit, again pedogenically modified before arrival of the basal lava flows. Overall the Lameta beds are considered to represent a regionally extensive Maastrichtian regolith.

Carbon and oxygen isotope analyses of calcareous components are entirely consistent with soil-zone environments. The $\delta^{13}C$ values are low, typically -8 to $-9‰$ PDB, demonstrating a strong input of carbon from the decay of terrestrial land plants. Calcrete $\delta^{18}O$ values are variable, -5 to $-10‰$ PDB consistent with precipitation from meteoric water, some of which was evaporatively modified in pools on the alluvial/palustrine flat.

The Lameta Beds are well known for sauropod nesting sites and sedimentological analyses of these sites suggest that the animals selected topographic highs, usually in marly or sandy, soft sediment. Multiple nests with similar egg types probably indicate colonial nesting. Isotopic analyses of eggshell carbonate agree with earlier work suggesting that the sauropods ate a "C3" plant food.

1. Introduction

Since the original discovery of dinosaur eggshells (Mohabey, 1983), a notable record of nesting sites has been documented from Maastrichtian strata associated with the Deccan Volcanics of central India (Sahni, 1989). The nests occur in calcareous rocks extending for over 1000 km along the E–W trending Narmada Valley (Fig. 1)—a major extensional feature of the Indian sub-continent (Varma and Banerjee, 1992). In the Jabalpur sub-region (Fig. 1) the nests occur as part of a more developed infratrappean sedimentary sequence known as the Lameta Beds. Five eggshell types (attributed mostly to titanosaurid sauropods) have been recognised on the basis of morphological characters (Sahni et al., 1994). The most important and well studied localities for nesting sites in the region are Anjar (Kachch), Balasinor (Kheda), Dohad, Hathni River (near Kukshi) and Bagh Caves, Jabalpur, Pisdura and Nand, Nagpur (Takli) (Fig. 1).

Palaeoenvironmental reconstruction of the Lameta Beds (Table 1) is important for under-

0031-0182/95/$9.50 © 1995 Elsevier Science B.V. All rights reserved
SSDI 0031-0182(94)00128-6

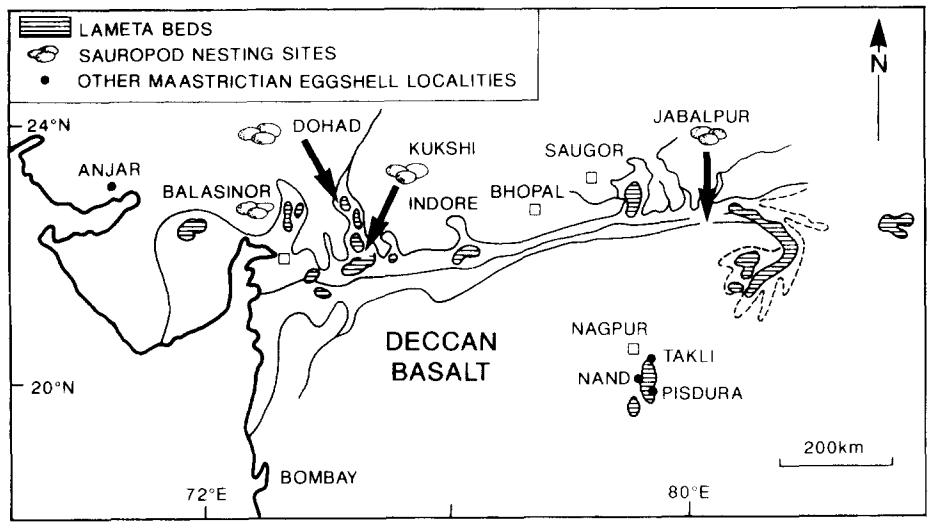

Fig. 1. Outline map of the Narmada region of central India showing the important Lameta Beds outcrop areas and important sauropod nesting sites. Other Maastrichtian sauropod eggshell localities are also marked.

Table 1
Stratigraphy of the Jabalpur sub-region

Late Cretaceous (Maastrichtian)	Deccan Flows Intertrappean sediments Deccan Flows Lameta Beds
	Unconformity
Mid-Jurassic to Early Cretaceous	Jabalpur Group (Channel Sandstones: overbank thin white to brown sandstones, fireclays)
	Unconformity
Precambrian	Mahakoshal Group (Meta-sedimentary sequence, complexly deformed) Granite basement

standing Maastrichtian palaeogeography at the initiation of volcanism in the eastern part of the Deccan volcano-sedimentary province and also for understanding sauropod nesting habits. Previous studies on the sedimentary environments of the Lameta Beds have focussed on the Jabalpur sub-region (Jabalpur city and a radius of ~50 km). Interpretations have varied from terrestrial (Medlicott, 1872; Matley, 1921) to shallow marine (Chanda, 1963a,b) to fluvial and shallow marine (Kumar and Tandon, 1977, 1978, 1979), and to tidal and estuarine environments (Singh and Srivastava, 1981; Singh, 1981). More recently, Brookfield and Sahni (1987) interpreted the Lameta Beds as continental deposits of a semi-arid region. Tandon et al. (1990) interpreted the Green Sandstone (see below) as fluvial deposits and the Lower Limestone and Mottled Nodular Beds (see below) as pedogenically modified from palustrine mudflats. Palaeoenvironmental studies on the Lameta Beds from other areas and sub-regions of central India suggest an alluvial-limnic setting (Joshi and Ganapathi, 1990; Mohabey et al., 1993). Mohabey and Udhoji (1990) concluded that the Lameta Beds of the Nand area in the Nagpur district were formed in an alluvial environment comprising overbank, channel and backswamp subenvironments.

This study aims to improve existing interpretation with detailed facies, petrographic and geochemical (carbon and oxygen stable isotope) data, to better understand the depositional and palaeopedologic conditions of the Lameta Beds.

2. Deccan volcanism

Towards the end of the Cretaceous, a major part of peninsular India (western and central) was

affected by large-scale volcanic activity resulting in the accumulation of a >2 km thick pile of tholeiitic lavas. These lava flows, the Deccan Traps, cover large areas of Kutch, Saurashtra, Gujarat, Maharashtra, Madhya Pradesh, Andhra Pradesh and Karnataka forming a total area of half a million square kilometres (Fig. 2). The present distribution of the lava pile is only a part of their former extent (Fig. 2), both areally and vertically, as a considerable volume was denuded in the Cenozoic. It is estimated that the lavas may have covered over 1.5×10^6 km^2 with a total erupted volume of 2×10^6 km^3 (Raja Rao et al., 1978; Courtillot et al., 1988).

Combined palaeomagnetic, palaeontological and geochronological data suggest that the Deccan lavas had an eruptive duration of 1 m.y., since volcanism did not exceed three *successive* magnetic chrons, (end of 30N, 29R and the beginning of 29N—see Courtillot et al., 1986). A 2000 m thick sequence of stratigraphically controlled and geochemically well characterised tholeiitic basalts of the Western Ghats, gave ^{40}Ar to ^{39}Ar ages of 66.8–68.5 m.y. (Duncan and Pyle, 1988). There was *no significant difference* in age from the stratigraphically oldest to the youngest rocks. In the last five years, radiometric ages, the N-R-N magnetostratigraphic sequence, and palaeoentological data have been combined to infer that the sequence of lavas resulted from extremely rapid eruptions

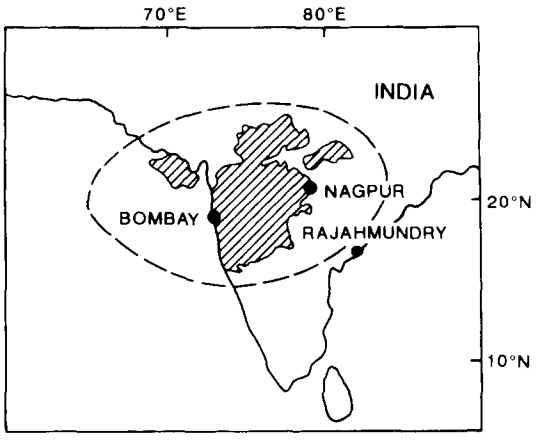

Fig. 2. Outline map showing the present (shaded area) extent and inferred former extent (pecked line) of the Deccan province.

at the Cretaceous/Tertiary (K/T) boundary (Jaeger et al., 1989; Courtillot et al., 1988). Viewed as a catastrophic event, the Deccan Volcanism has been causally linked to mass extinctions at the K/T boundary (McLean, 1985).

However, the interpretation of the Deccan volcanism as a short-lived catastrophic event is not universally accepted. Very recently, Jaiprakash et al. (1993) have shown from an offshore well (PLKA), off the eastern coast near Rajahmundry that the lava flows are interbedded with sediments ranging in age from M-19 planktonic zone (66.5–65.5 Ma) to P-2 zone (61.2–60.7 Ma). Further, Venkatesan et al. (1993) provide strong evidence that a 1.8–2 km thick bottom segment of the exposed basalt flow sequence in the Western Ghats was extruded within a very short time ($\sim$1 m.y.) close to 67 m.y. However, the upper section, consisting of the Ambenali Formation and the Mahabaleshwar Formation has mean plateau and isochron ages of 62.3 ± 2.4 m.y. On the basis of these data, Venkatesan et al. (1993) concluded that the basal section of the Deccan Volcanics in the Western Ghats is distinctly older than the K/T boundary. These new results argue for a longer duration (6–7 m.y.) of Deccan Volcanism. Thus, while the Deccan Volcanism may have been temporally connected to K–T events, it may not have been a catastrophic event of $\sim$1 m.y. duration coincident with the K/T boundary (Jaiprakash et al., 1993; Venkatesan et al., 1993).

The infratrappean Lameta Beds are palaeontologically indistinguishable from intertrappean sedimentary successions (Sahni and Jolly, 1990). Further, the Green Sandstone (Fig. 3)—the basal unit of the Lameta Beds in Jabalpur—contains a clay mineral assemblage of montmorillonite, celadonite, illite and kaolinite (Tandon et al., unpublished results). Montmorillonite and celadonite represent the degradation of parent basaltic materials, suggesting presence of volcanogenic detrital constituents in the basal Lameta Beds. Consequently, the sauropod nesting sites of central India, occurring in the sandy carbonate lithofacies (Lower Limestone/Mottled Nodular Beds) overlying the Green Sandstone, *post-date* the initial eruptive activity in the region. In the Anjar locality (Kachch) (Fig. 1), Bajpai et al. (1990) recorded both sauropod and ornithoid eggshell morpho-

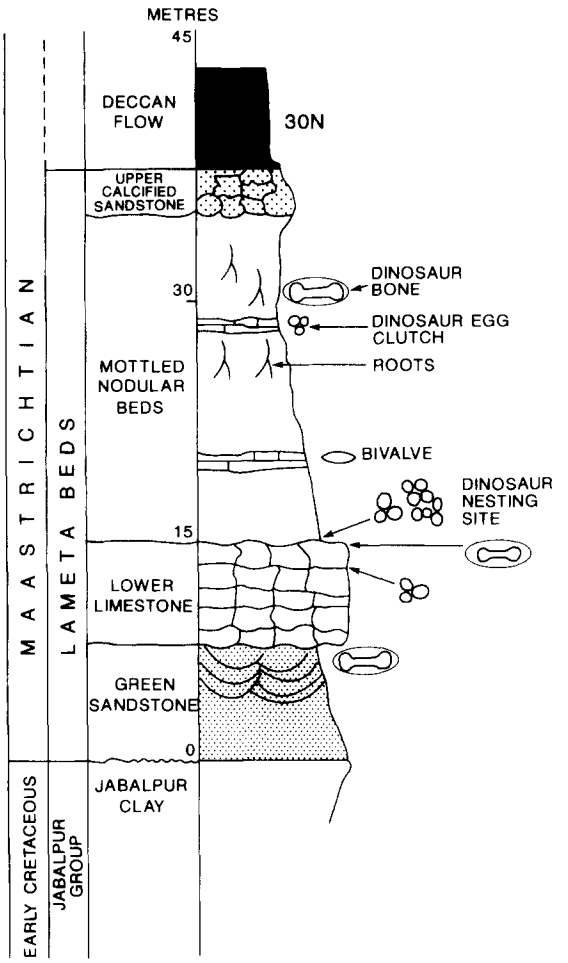

Fig. 3. Main stratigraphic sub-divisions of the Lameta Beds of the Jabalpur sub-region. Note the dominant occurrence of nesting sites in the Lower Limestone. Partially articulated dinosaur skeletons occur in the Lower Limestone. Dinosaur bones occur both in the Green Sandstone and the Mottled Nodular Beds.

types in sediments occurring between two flows confirming that dinosaur nesting occurred in association with the initial eruptive phases.

3. Late Cretaceous strata of the Narmada Valley

The Late Cretaceous strata of the Narmada Valley are represented by the Bagh Beds, Lameta Beds, Deccan Volcanics and intertrappean sedimentary sequences (Blanford, 1869; Pascoe, 1964). The Bagh Beds are confined essentially to the western segment of the >1200 km long valley and consist dominantly of calcareous facies. Two persistent lithological units—the Nodular Limestone and the Coralline Limestone—occur widely. The Nodular Limestone is fossiliferous in its upper part, and contains bivalves, bryozoa, gastropods and ammonites. Singh and Srivastava (1981) attribute the nodular character to the presence of *Thalassinoides* burrows. The locally developed Deola Marl contains echinoderms, bryozoa, bivalves, brachiopods, ammonites, shark teeth, ostracodes (Chiplonkar et al., 1977) and planktonic foraminifera (Sharma, 1976). The Coralline Limestone is a cross-bedded (large-scale ~1 m thick) calcarenite made up of skeletal detritus—mostly bryozoan fragments. Based on ammonoids, the Bagh Beds are assigned a Turonian age (Pascoe, 1964) although their exact age is disputed (Robinson, 1967; Sahni, 1984).

In contrast to the (?) Turonian marine Bagh Beds, the infratrappean beds (Lameta Beds) occur, in patches, *all along* the Narmada Valley. They are particularly well developed in the eastern part of the valley (for example, Jabalpur sub-region, Saugor sub-region). Numerous occurrences are known from the Amarkantak, Mandla, Jabalpur, Saugor district in the upper and middle reaches of the Narmada Valley (Fig. 1). Further to the west and in the lower reaches of the Narmada Valley, the Lameta Beds may occur in association with the Bagh Beds or may directly overlie Precambrian basement (Roychaudhri and Sastry, 1962).

It has been suggested that the Bagh Beds and Lameta Beds are synchronous (Blanford, 1869); the former representing marine and the latter freshwater environments. Raiverman (1975), Singh and Srivastava (1981) and Singh (1981) subscribed to this view, the latter workers suggesting a tidal estuarine origin.

However, Roychaudhri and Sastri (1962), based on detailed geological mapping, concluded that the Lameta Beds, where they are in contact with the Bagh Beds, overlie them unconformably. This observation is in agreement with the reassigned Maastrichtian age of the Lameta Beds (Buffetaut, 1987; Sahni and Bajpai, 1988; Jaeger et al., 1989).

Table 2
Stratigraphy of the Lameta Beds of Jabalpur, central India

Matley (1921)		Chanda and Bhattacharya (1966, 1968)		Singh and Srivastava (1981)	This study	
Deccan Traps		[d]Deccan Traps		Deccan Traps	Deccan Traps	
Lameta Group	(e) Upper Sands	[c]Lameta Group	(c) Upper Sandy Limestone	Limestone Upper Sandstone	Upper (calcified) Sandstone	
	(d) Upper Limestone (local zone)		(b) Lower Limestone	Mottled Nodular Beds	Mottled Nodular Beds	
	(c) Mottled Nodular Beds		(a) Green Sand	Lower Limestone	Lower Limestone	
	(b) Main or Lower Limestone	**——Disconformity——**		Green Sandstone	Green Limestone	
	(a) Green Sand	[b]Jabalpur Group	(c) White Clays	Jabalpur Group	**——Unconformity——**	
			(b) Sandstone		(b) White Clays	(a) Sandstone
			(a) Silty Clays			
		——Non-conformity——				
		[a]Precambrian Granites and Schists				

4. Stratigraphy of the Lameta Beds

In the Jabalpur sub-region where the Lameta Beds are thickest (~50 m), they unconformably overlie a range of Mesozoic-Precambrian rocks (Table 1; Fig. 3). Where the Lameta Beds overlie the mid-Jurassic to Early Cretaceous Jabalpur Group, they do so with paraconformity in the east Jabalpur region, passing into erosional unconformity toward the south-west (Chanda and Bhattacharya, 1966).

The Lameta beds were originally sub-divided into five mappable units in the Jabalpur region (Matley, 1921) (Table 2). However, Chanda and Bhattacharya (1966) suggested integration of the upper three units (Mottled Nodular Beds, Upper Limestone, Sandy Zone), into a unit designated as the Upper Sandy Limestone because of the lack of sharp mutual contacts between units and lateral impersistence (Table 2).

In the Jabalpur area the Upper Limestone is a compact and indurated calcareous sandstone (Chowdhury, 1963; Singh and Srivastava, 1981; Tandon et al., 1990). The Upper Sand of Matley (1921) occurs as a small patch (not mappable) beneath volcanic debris at the Bara Simla Hill. Elsewhere, at Lametaghat, Burgi, Amkoh, and Silondi in the Jabalpur sub-region, the Mottled Nodular Beds are succeeded by a white to buff friable quartzose sandstone (Fig. 3). In the Jabalpur sub-region, there is only one unit which succeeds the Mottled Nodular Beds—a calcified sandstone/sandy calcrete or a white to buff trough cross-bedded quartzose sandstone (Fig. 3). We follow a four-fold sub-division (Table 2). The lower three units of Matley (1921) are retained while the Upper Limestone and Sandy Zone of Matley are replaced by Upper Calcified Sandstone/Sandy Calcrete. The Lameta beds are overlain by the lower Deccan flows.

5. Fauna/flora of the Lameta Beds

Diverse freshwater and terrestrial faunas/floras such as dinosaur skeletal remains and eggshells, molluscs, ostracodes, pollen and charophytes are known from the Lameta Beds (Huene and Matley, 1933; Matley, 1923; Sahni, 1984; Sahni and Mehrotra, 1974; Bhatia and Rana, 1984; Bhatia et al., 1990; Dogra et al., 1988).

The dinosaurian remains, occurring in the sandy and pebbly marls of the Lower Limestone, are most well known (Buffetaut, 1987). *Titanosaurus* including *T. indicus* and *Antarctosaurus septentrionalis Huene* are reported from the sauropod bed at the base of the Lower Limestone (Huene and Matley, 1933). *Titanosaurus* and several theropods including *Indosuchus, Compsosuchus, Laevisuchus, Coeluroides, Lametasaurus* are reported from the "carnosaur" bed lying above the limestone.

These beds have also yielded freshwater aquatic pulmonates including *Paludina, Physa* and *Lymnaea*, ostracodes including *Cyprinotus, Paracypretta, Eucandona* and *Darwinula*, and charophytes including *Microchara, Peckichara* and *Platychara* (Sahni and Jolly, 1990). Microvertebrate remains include scales of *Phareodus*—an osteoglossid fish, *Lepisosteus, Pycnodus, Apateodus, Stephanodus*, and a species of frog belonging to the family Pelobatidae (Sahni, 1984; Brookfield and Sahni, 1987; Sahni et al., 1994). *Igdabatis*—a myliobatid is also reported (Besse et al., 1986; Courtillot et al., 1986) from the Upper Sandstone unit at Burgi.

The pollen assemblage recorded from the type area of the Lameta Beds is a typical Maastrichtian association of angiosperms, gymnosperms and pteridophytes including *Ariadnaesporites punctatus, Leptolepidites verrucatus, Proxapertites crassimurus, Palmidites maximus, Liliacidites microreticulatus, Aquilapollenites indicus, A. bengalensis, Aquilapollenities andamanensis, Scollardra conferta* and *Dinogymnum* sp. (Dogra et al., 1988).

Earlier reports of foraminifera in the Mottled Nodular Beds of Jabalpur (Kumar and Tandon, 1977) have not been confirmed by subsequent work. Similarly, supposed thalassinid burrows from the Mottled Nodular Beds (Kumar and Tandon, 1977) and Green Sandstone (Singh, 1981) were probably misidentified pedogenic calcrete nodules (Brookfield and Sahni, 1987). Those bur-

rows which are genuine might equally have been made by a soil dwelling fauna.

6. Age of the Lameta Beds

The Lameta Beds were originally assigned a Turonian age based on the dinosaurian faunas (Huene and Matley, 1933). However, comparison of dinosaur faunas of the Lameta Beds with well dated dinosaur faunas from other parts of the world is difficult, and there is no firm evidence to refer them to the Turonian (Buffetaut, 1987). Re-assessment of the biochronology of the dinosaurian faunas of the Lameta Beds (Chatterjee, 1978; Colbert, 1984), the presence of *Igdabatis* (Besse et al., 1986), *Aquilapollenites* sp. (Dogra et al., 1988) and palaeobatid frogs are used to infer a Maastrichtian as opposed to Turonian age.

The age of the Lameta Beds has a bearing on the age and duration of Deccan Volcanism—particularly as the basal Green Sandstone contains volcanogenic detrital montmorillonite and celadonite inferred to be derived from Deccan Traps (Kohli, 1990). Analysis of the microvertebrates of the infratrappean and intertrappean sequences shows that the biotic assemblages of the two are indistinguishable (Prasad, 1989; Sahni, 1984). Also Sahni et al. (1994, p. 204) point out that the terms "infratrappean" and "intertrappean" describe the local physical position of the beds in relation to lava flows regardless of chronology.

In summary, the grouping of the Lameta Beds with the basal Deccan flows and intertrappean sedimentary sequences is consistent with data obtained from recent biochronological, radiometric and mineralogical investigations. The Deccan volcanics and associated infratrappean (Lameta Beds)—intertrappean sedimentary sequences are assigned to a Maastrichtian–Danian interval ($\sim$60–$\sim$70 m.y.) and include the K/T boundary.

7. Dinosaur eggs and nesting sites

Dinosaur eggshells and nesting sites are found in both infra- and intertrappean sequences, but are common in the indurated, mottled, nodular, sandy calcrete of the Lower Limestone. In the Jabalpur sub-region, there is only one instance of an egg clutch occurring in the Mottled Nodular Beds at the Lametaghat (south bank) section.

Here, the term "nesting site" or "nest" specifies the association of at least two or more eggs in close juxtaposition signifying the original pattern of laying. Eggshell fragments are found as isolated specimens in screen-washed materials yielding microvertebrates and other microfossils. The nesting has been attributed mainly to titanosaurid sauropods. Five eggshell types (Table 3) have been recognised on the basis of morphological characters (Sahni et al., 1994). Most of the eggs in the nests are apparently unhatched, and in no instance are embryonic remains preserved.

In the Jabalpur sub-region, nesting sites have been recorded from the Bara Simla Hill, Chui Hill, Lametaghat (north bank) and Lametaghat (south bank). At Bara Simla Hill, nine "nests" were recorded in an area of 100×50 m. Most eggs in the nests have a roughly circular outline and tend to occur in the "detritus rich patches" of the sandy calcrete. Individual eggs in nests or isolated eggs without exception exhibit in situ fragmentation (Sahni et al., 1994) but original sphericity and size is retained. The eggs usually have diameters of 14–18 cm, but in an exceptional case, a diameter of 28 cm was recorded from Bara Simla Hill.

8. Sedimentology and lithofacies of the Lameta Beds

Lithofacies, petrographic and geochemical data are centred on the Lameta Beds of the Jabalpur sub-region. However, additional observations on palustrine limestones of the Saugor sub-region (Fig. 1) and the Bharela intertrappean Beds are included to clarify interpretations. The isotopic composition of a few sauropod eggshells and host calcretes from Kukshi and Balasinor (Fig. 1) in the western segment of the Narmada Valley are similarly included.

8.1. Green Sandstone

The Green Sandstone, 3–10 m thick, consists of green and white, medium to coarse grained and

Table 3
Sauropod eggshell characters (after Sahni et al., 1944) of the Narmada region

Eggshell type	Characters
1. Titanosaurid type I	Eggs spherical, usually 14–18 cm diameter, wall thickness 2–3.5 mm; single layered, spherulitic, shell units long, compressed, cylindrical in shape and separated, shell unit boundaries parallel, mammillae caps small, pore canals long, narrow resembling tubocaniculate type; extinction pattern sweeping; outer surface with circular or subcircular, well separated nodes, subcircular pores on outer surface; inner surface with subcircular mammillae, 0.2–0.5 mm in diameter
2. Titanosaurid type II	Eggs spherical, 14–18 cm diameter, wall thickness 1–1.5 mm, single layered spherulitic, shell unit compressed, usually conical and/or cylindrical, discrete, pore canals long narrow vertical or sub-vertical and of tubocanaliculate, inner surface with mammillae distinctly smaller than Type I, mammillae tightly packed
3. Titanosaurid type III	Eggs spherical, 14–20 cm diameter, shell thickness 1.0–1.5 mm, single layered, spherulitic; shell units discrete or partially fused, growth striations coned towards the base; pore canals narrow and curved, often incomplete, herring-bone pattern well developed, extinction pattern sweeping; inner surface with isolated or coalescing mammillae of variable diameter (0.15–0.30 mm)
4. Ornithoid type	Eggshell two layered, thickness 0.4–0.5 mm, mammillary layer thick, mammillary cones distinct, radiating and tightly packed; horizontal layering observed in rare instances, no abrupt change from mammillary to continuous layer; extinction pattern columnar; outer surface with irregularly spaced tubercles; inner surface with tightly packed mammillae (diameter 0.03–0.05 mm); pores not visible on the outer surface
5. Indeterminate type Dinosauria	Eggshells thin 0.1–0.4 mm, single layered spherulitic, shell units discrete and usually conical in shape; growth striations arched; outer surface with discrete nodes; mammillae well developed, subcircular

pebbly, trough cross-stratified sandstones. These are mainly composed of angular to subrounded quartz grains. Green interstitial clay, where present, varies from 1 to 9% (Verma, 1965). Large, medium and small-scale trough cross-bedded sandstones, channel scours, channel lag deposits, and horizontal laminated muddy sandstone are common features (Fig. 4).

Individual co-sets of trough cross-beds in medium to coarse grained sandstone measure up to 1 m. Groups of co-sets are truncated by erosional surfaces. For example, at Chui Hill an undulating contact between the Jabalpur Clay and the Green Sandstone constitutes a basal erosional surface. Within the Green Sandstone, major erosional scours up to 2 m deep are well developed, filled by medium to coarse-grained sand and in one instance by mudstone. Of the three erosional surfaces at Chui Hill, well developed lag deposits occur only in the upper one. These consist of clasts up to 25 cm across, lying without specific orientation in the coarse sand, and make up the basal 50 cm of the bed. The larger clasts consist of sandstone, clay and reworked calcrete nodules, mostly derived locally—some of them intraformationally. The smaller clasts consist of vein quartz, black chert and jasper derived from older metasedimentary sequences of the region. Palaeoflow directions determined at various localities (Bose, 1992) show unimodal distributions with a predominant SW transport. Foresets are generally inclined between 20–25°, but exceptionally up to 34°.

The other important facies association is a 7 m thick upward-fining unit of coarse to very fine grained friable white sandstone. Sedimentary structures within this unit pass from large-scale trough cross-beds (metre scale) into medium-scale trough cross-beds (30–50 cm) and small-scale trough cross-beds ($\sim$5 cm) eventually passing into a laminated mudstone. A few isolated planar cross-beds also occur. Rib and furrow structures are observed on some siltstone bedding surfaces of the upper part of the cycle. Palaeoflow directions,

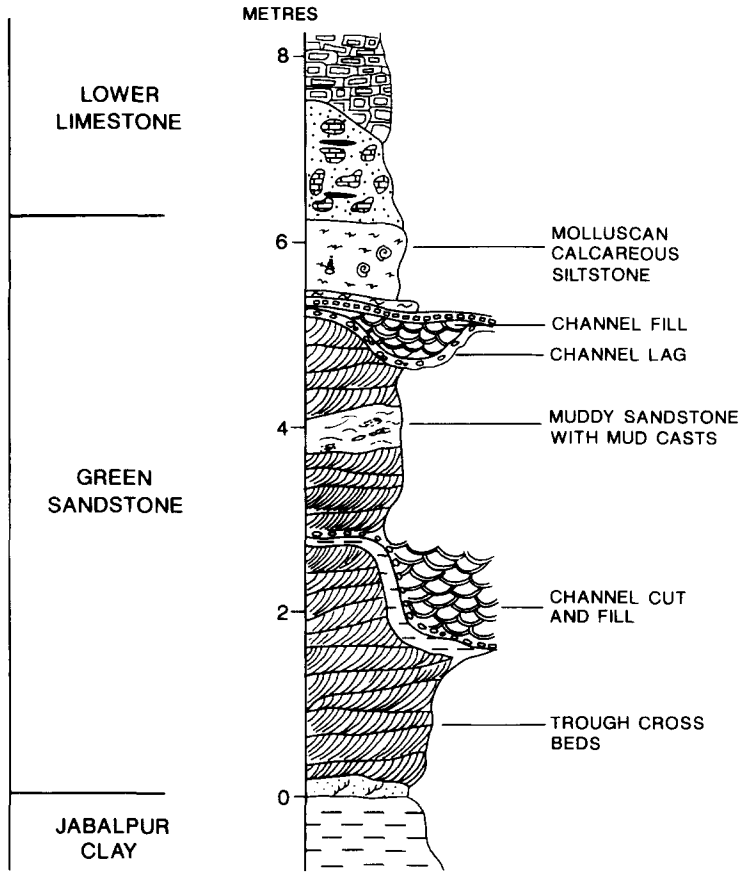

Fig. 4. Facies log showing trough cross-bedded sandstone, scour surfaces, channel lag and channel fill sandstone. Note laterally discontinuous thin muddy sandstone and a few green mudstone clasts in the trough cross-bedded sandstone facies.

determined from medium- and large-scale trough cross-stratified sets, vary from S to W.

Apart from these two major facies associations, parallel laminated units, <50 cm thick, of muddy sandstone, mud drapes, thinly inter-laminated mudstone and sandstone, occur with the groups of trough cross-beds. These units are lenticular and laterally discontinuous. Penecontemporaneous erosion of these layers is indicated by the occurrence of small mud clasts within the sandstones.

At Chui Hill, a contrasting association of low angle cross-bedding, horizontal bedding and channel lag deposits constitutes the upper part of the Green Sandstone, whereas the lower section consists of large to medium trough cross-stratified sandstones with at least two prominent erosional surfaces.

Petrologically, the Green Sandstone consists of texturally immature (angular to sub-rounded) and compositionally mature (quartzose) sandstones. Green clays occur in interstitial spaces, as skins around framework grains, and also as grain coating. Large micas, showing variable degrees of alteration, are present. The green clays consist of a multimineralogic assemblage of montmorillonite, celadonite and kaolinite (Kohli, 1990).

8.2. Interpretation

The association of groups of co-sets of large and medium scale trough cross-beds truncated by

erosional surfaces clearly indicate the presence of migratory bedforms in a channel belt. Further, the association of mud drapes, erosional surfaces, parallel laminated muddy sandstone and shale chips suggest strong stage fluctuations in the channels—or ephemerality. Occasional mud-filled channels support ephemerality, suggesting channel cutting, abandonment of cuts, and subsequent mud-filling. The facies association of fining upward sandstones suggests locally sinuous and (?) meandering channel patterns. Values of the dihedral angle of foresets (between 20–25°) but in places up to 34°, might suggest aeolian influence during subaerial exposure of channel bars.

Overall, we interpret the Green Sandstone as two to three storied sand accumulations in south-west oriented fluvial channels. These channels were shallow, braided (low-sinuosity), and show evidence of stage fluctuations. The occurrence of groups of co-sets of trough cross-beds associated with parallel laminated muddy sandstone, the presence of laterally impersistent erosional surfaces, and the low variance of directional data support a braided channel pattern. Green mudstone intraformational pebbles were probably incorporated from the desiccation and reworking of mudstone layers (Rust, 1978; Allen, 1983). Ephemeral stream deposits, or those formed in streams with markedly low stage conditions which are characterised by aggradation rather than lateral accretion (Glennie, 1970; Picard and High, 1973; Stear, 1985) are good modern analogues. Internal erosional surfaces covered with intraformational clasts are probably indicative of pulsatory flows during a single sandy ephemeral flood (Stear, 1985). This interpretation is consistent with the occurrence of reworked calcrete nodules in the channel lag deposits.

The Green Sandstone has been variously interpreted as a shallow marine deposits (Chanda, 1963a,b, 1967; Chanda and Bhattacharya, 1966), as point bar deposits (Kumar and Tandon, 1977), as estuarine channel deposits (Singh et al., 1983), and as semi-arid river system deposits (Brookfield and Sahni, 1987). Reasons for discounting a marine origin have already been discussed (Brookfield and Sahni, 1987) and our observations support their interpretation.

8.3. Lower Limestone

This is a regionally persistent unit and consists of impure cherty limestone, locally with abundant sand and small pebbles. Abundant chert segregations, mostly as irregular lenticles, occur within the limestone. In some areas, such as the Linga area of the Chhindwara district of Madhya Pradesh, the Lameta Limestone appears to be a mere calcification of the upper surface of the subjacent gneiss (Fermor and Fox, 1916 in Pascoe, 1964). Clearly a soil-zone origin was suggested, although modern pedological terminology was not applied until the study of Brookfield and Sahni (1987).

The Lower Limestone is 3–15 m thick in the Jabalpur sub-region. The contacts of the limestone with the underlying Green Sandstone and overlying Mottled Nodular Beds are irregular and undulose, accounting for the thickness variation. Several facies and subfacies occur in the Lower Limestone as outlined below and in Fig. 5.

(1) *Palustrine limestone facies* is a dense, compact micrite. Although apparently homogeneous, polished slabs show thin cracks, and development of a fragmented character through autobrecciation (Freytet and Plaziat, 1982). The limestone shows abundant silica stringers which occur as crack fills. Pebbly and sandy detritus occurs chaotically within the limestone often as mechanical fills of crack systems.

Non-orthogonal and orthogonal shrinkage cracks are common forming incomplete or complete polygons. The cracks are either subhorizontal or subvertical (Fig. 6). Variations within the oriented orthogonal crack system include both rectilinear (Fig. 7) and prismatic patterns (Fig. 6). In vertical faces, some shrinkage cracks show uniform width over a few tens of centimetres. However, in most cases the preserved patterns are complex because of overprinting by succeeding episodes of shrinkage. Shrinkage features show considerable variation in width from one millimetre to several centimetres.

Crack infilling is mostly of the bridge simple type (Allen, 1982), the fill being either of mechanical or chemical origins, or mixed. Collapse of the shrinkage features has resulted in cannibalism of

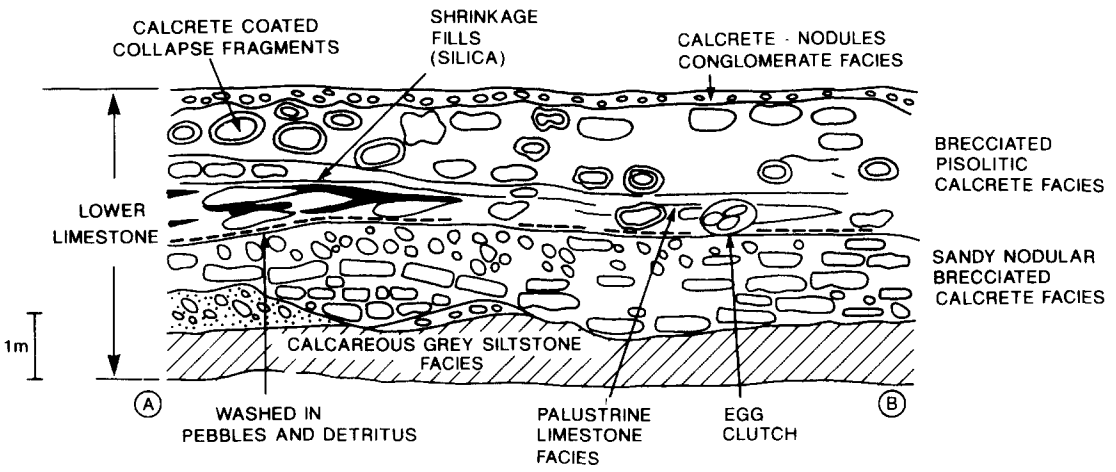

Fig. 5. Schematic diagram (exaggerated vertical scale) of the Lower Limestone in a vertical face of the Chui Quarry. Note the rapid lateral variations in the facies, and the occurrence of the sauropod egg clutch in the detritus rich area of the calcareous facies. Horizontal distance between A and B = ~20 m.

materials from the walls of the cracks. These are preserved as sandy brecciated calcretes with collapse fragments of buff microcrystalline limestone. They are of highly irregular three-dimensional form, and may extend up to a few metres. This results in an intimate association of buff fine grained limestone and shrinkage infilling sandy calcretes of variable form (prismatic, rectilinear, irregular).

(2) *The sandy, nodular, brecciated calcrete facies* is a compact, detritus-rich, microcrystalline carbonate. Abundant pebbles of chert, jasper, quartz and sand-sized detritus occur in variable proportions within the calcrete. Nodules vary from a few millimetres up to several centimetres diameter and are of irregular shape. The nodules show internal cracks and consequently display "nodule in nodule" patterns. Brecciation is common, and in most outcrops, multiple episodes of shrinkage and related brecciation are recognised. Contemporaneous with shrinkage and related brecciation was the infilling of newly formed spaces by cryptocrystalline silica.

Multiple episodes of shrinkage, brecciation and crack-filling are indicated by several mutually discordant patterns of silica healed cracks, particularly those cutting across previous generations of breccia fragments. Further, intrastratal reworking, including rotation of older "breccia fragments", is indicated by the cross cutting relationships between crack fills of adjacent fragments.

In places, these nodular-brecciated calcretes show mottling–mostly red brown diffuse mottles of irregular size and shape. Meniscate burrows also occur mainly in the sand rich patches of the calcrete. Similarly, sauropod nests also occur in the sand rich areas of the calcrete.

(3) *The calcareous grey siltstone with brecciated calcareous nodules* is a locally developed facies (Chui Hill) and has yielded an assemblage of freshwater aquatic pulmonate gastropods and charophytes (Sahni and Jolly, 1990). Nodule abundance increases in the upper part of the facies. The nodules are brecciated, and in places, show diffuse grey mottles.

(4) *The brecciated-pisolitic calcrete facies* is locally well developed in the upper part of the Lower Limestone of the Chui Hill. It consists of a brecciated and fragmented calcareous facies with abundant circumfragmental envelops of a "dirty ochre" coloured carbonate. The shapes of the coated fragments vary from rectangular blocks to accretionary pisoidal structures with small nuclei, and measuring a few centimetres in diameter. The accretionary envelops follow the outline of the fragment. In some pisolitic structures, discordant

Fig. 6. Outcrop photograph (Chui Quarry) of vertical face of buff palustrine limestone showing well developed shrinkage cracks. Cracks filled with sand (now sandy calcrete). Also, note the very well developed prismatic pattern resulting from the dominant vertical/subvertical cracks.

laminae are observed and imply intrastratal rotational translocation of fragments during their growth. The forms of individual elements in the brecciated-pisolitic calcrete are related to shrinkage patterns, degree of local reworking within the horizon, and modification of the external outline of the fragment through subsequent shrinkage, and in places renewed fragmentation.

(5) *The honeycomb calcrete facies* occurs locally in association with buff fine-grained limestone and shrinkage infilling sandy calcretes of variable form. The honeycomb structure is made up of a very fine mesh of intersecting veins of white calcite spar woven within a grey calcrete. This facies, because of its peculiar appearance, stands out prominently as irregular patches within the buff fine grained limestone. The morphology is also comparable to the "chickenwire" texture associated with evaporitic minerals; however, no evidence for replacement of precursor evaporitic minerals is available.

(6) *The sandy and pebbly green marl* is a laterally impersistent facies and consists of green siliceous marl with locally abundant arenaceous material. In places, the rock is a conglomerate and consists of black chert, vein quartz, jasper and reworked intraformational clasts consisting of calcareous nodules and green mud clasts. Fragmented dinosaur bones are associated with the clasts and articulated sauropod skeletons are also known (Chatterjee, 1992).

(7) *The calcrete-nodule conglomerate* facies is predominantly made up of intraformational clasts of reworked calcrete and palustrine limestone. Maximum clast size is up to 10 cm; the clasts vary in shape from subangular to subrounded. Extraformational clasts are less common, and smaller. Some of the reworked pedogenic clasts show gradations from calcrete to sil-calcrete. The matrix is calcareous sand, locally cemented by silica.

8.4. Petrography of Lower Limestone

In thin section these calcareous lithofacies reveal microcrystalline calcite with abundant floating detrital grains (Fig. 8), and linear cracks and void spaces filled with detrital grains and calcite spar and/or silica. Replacement of calcite by silica in large cavities is also common.

Other fabrics include patches of clotted micrite in the groundmass and nodulation of the micrite caused by contemporaneous shrinkage. The detrital grains are mostly quartz which, in several lithologies, particularly calcareous rhizocretions, show circumgranular envelopes of tangential spar/microspar crystals. The outline of these quartz grains is irregular and reflects etching and replac-

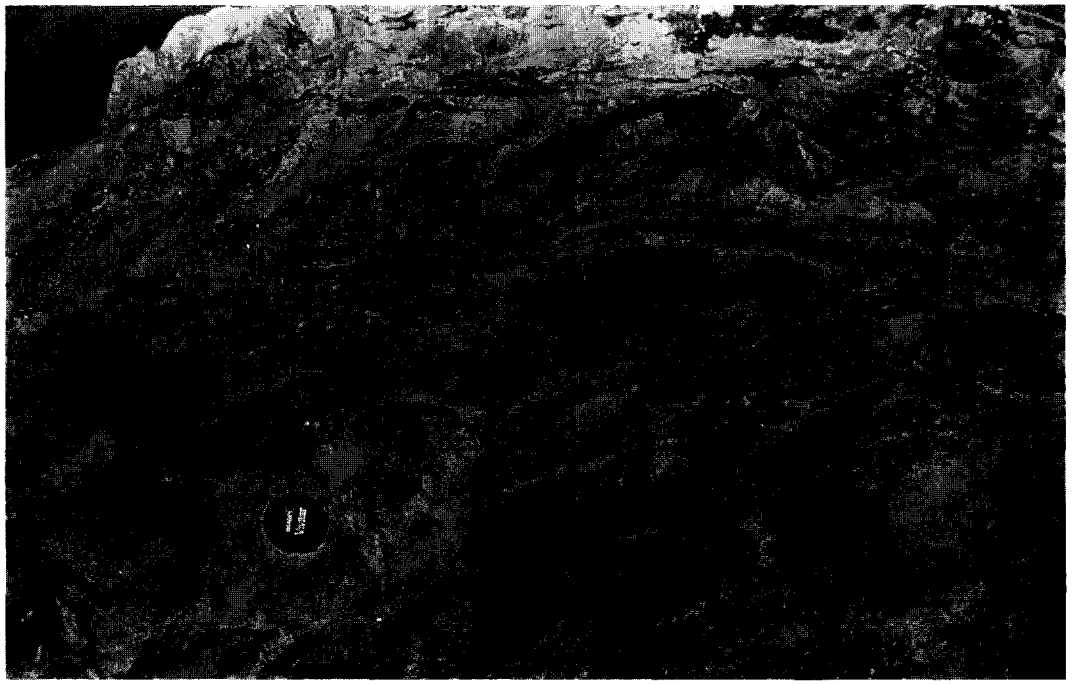

Fig. 7. Brecciated and nodular calcrete and palustrine limestone lithofacies showing abundant rectilinear fragments. Most fragments are coated and some have been affected by multiple episodes of coating.

ment by calcite (Nagtegaal, 1969; Wright and Tucker, 1991). Microspar rims around framework grains are, in some cases, asymmetrical and elongate downwards. Such gravitational features are common, but non-diagnostic, features of calcrete facies (Esteban and Klappa, 1983).

Calcareous glaebules (Brewer, 1976) are important constituents, and consist both of nodules with an undifferentiated internal fabric and vadoids with a concentric internal structure. Nodules with both diffuse boundaries (orthic nodules), and with sharp boundaries (disorthic) are recognised in the calcrete facies; the latter are attributed to movement caused by soil pedoturbation (Wieder and Yaalon, 1974).

The calcareous glaebules are cross cut by linear cracks, indicating that these were nonlithified and formed near surfaces affected by desiccation. Nodules also show internal wedge shaped crack patterns filled by sparry crystal mosaics. These resulted from drying and differential cementation between the interior and the exterior of the nodule and the surrounding soil matrix (Blodgett, 1988), and are indicative of calcrete facies (Esteban and Klappa, 1983). Some long and straight sided bands of spar with sharp, parallel margins, represent passive infilling of cracks with little or no crack wall modification. Multiple episodes of cracking are recognised by the superposition of later crack generations over pre-existing ones. In some facies, these shrinkage features comprising parallel systems gave rise to various (including quadrilateral) peds.

Disrupted, unsupported clastic grains result from the displacive growth of calcite in the micropores, re-entrants, fractures or other zones of weakness in grains (Watts, 1978; Braithwaite, 1989; Saigal and Walton, 1988; Buczynski and Chafetz, 1987).

Secondary silica and chalcedony is present as crack infills in both the calcrete and buff microcrystalline limestone. From the crack wall, a progression from microcrystalline quartz to chalcedony to megaquartz is common and spherulites of chalcedony (Fig. 9) occur in other cavities. Some of the framework grains rimmed by calcite

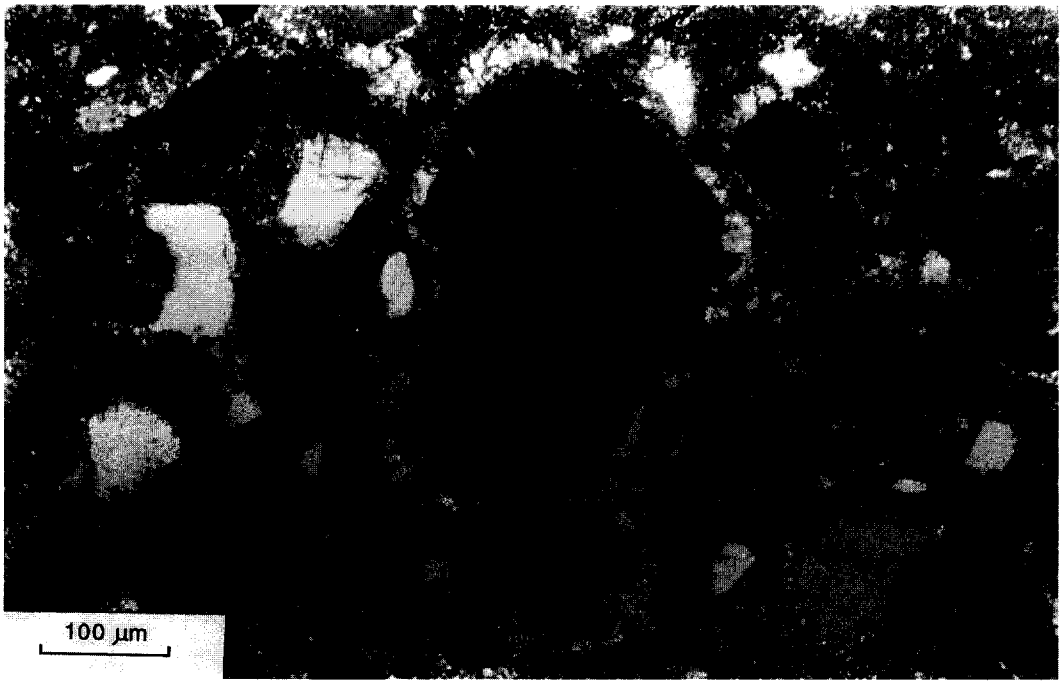

Fig. 8. Photomicrograph of calcareous nodule from sandy nodular calcrete (Lower Limestone) showing a floating fabric (quartz and felspar grains in a microcrystalline crack fill) around the felspar grain in the centre of photograph.

also show either partial or total replacement by chalcedony or microquartz.

8.5. Interpretation

The characteristic attribute of the calcareous lithofacies of the Lower Limestone is shrinkage, which is reflected by the development of multiple generations of cracks, related brecciation fabrics and micro-relief (Goldbery, 1982). Collectively, the Lower Limestone facies and their lateral variations in associations and thickness indicate a subaerially exposed low gradient alkaline flat in an alluvial setting. Small topographic differentiation allowed calcrete formation on relative highs and palustrine limestone and marl formation in relative lows of the plain (Sahni et al., 1994). These conditions, because of frequent and intermittent periods of desiccation, do not exclude the intimate association of calcrete and palustrine facies.

Shrinkage cracks are the result of volume changes within unlithified sediment, and common processes responsible for them are desiccation and synaeresis (Allen, 1982). The morphology, dimensions and patterns of those described here suggest formation by desiccation on subaerially exposed surfaces. They bear no resemblance to subaqeously formed shrinkage cracks (Donovan and Foster, 1972) or to those formed by other mechanisms (Kidder, 1990; Cowan and James, 1992). Clearly, this intermittently-desiccating subaerial exposure surface was connected to a fluvial system, demonstrated by several sandy/pebbly detritus dispersal events on the fissured ground.

Palustrine carbonates are shallow freshwater deposits showing evidence of both subaqueous deposition and subaerial exposure (Platt and Wright, 1992). Originally, Freytet (1973, p. 38) used the term for "lacustrine muds which may have emerged and come under the influence of vegetation and oscillations of the water table". Freytet and Plaziat (1982) envisaged these deposits as the marginal facies of a lacustrine system. Although the typical palustrine carbonate association of brecciated carbonate mudstones, pedogenically modified limestones with mottles, and biotas

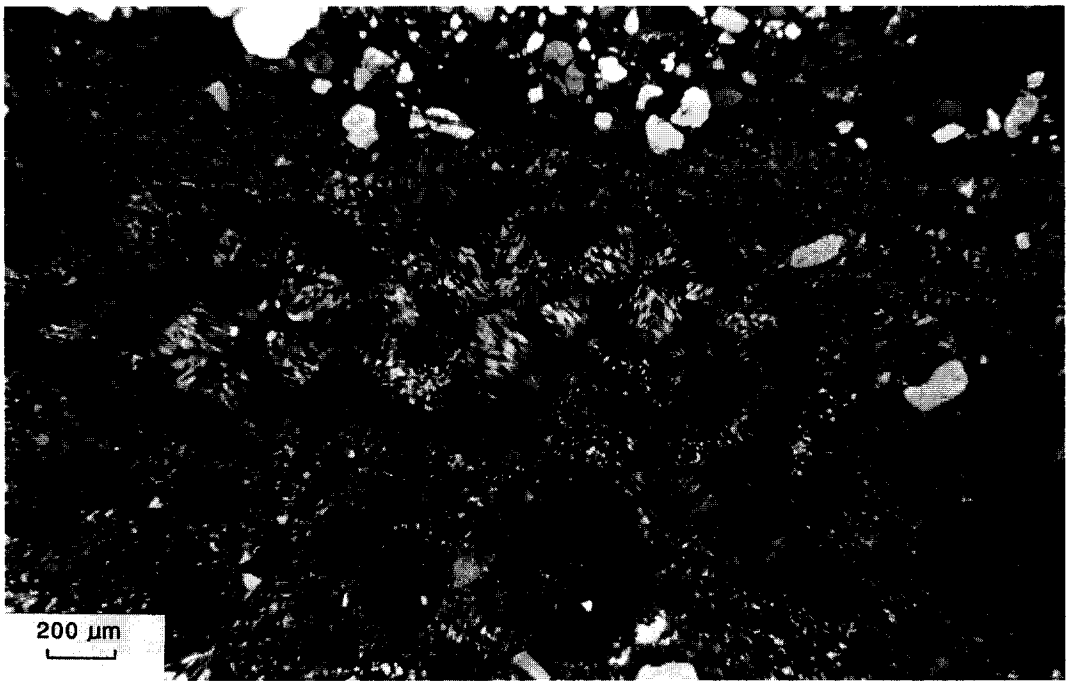

Fig. 9. Photomicrograph of palustrine limestone/calcrete facies showing a cavity filled with spherulitic chalcedony. Micritic glaebules present below the cavity and a grain rich area occurs above it.

of charophytes, ostracodes and gastropods are present in the Lower Limestone, profundal lake deposits and sublittoral facies are absent. The absence of "deeper" water facies in ancient palustrine successions has been discussed by Platt and Wright (1992) who noted that the modern Florida Everglades consist of extensive, very shallow carbonate marshes.

The palustrine limestones of the Lameta Beds represent a much smaller-scale system than the Florida Everglades and occur as laterally discontinuous units, a few square kilometres in area associated with alluvial sandstones, mudstones and palaeosols. The dominance of shallow water deposits with the virtual absence of "deeper" facies, and the repeated intercalation of thin discontinuous pebble layers suggests intermittent periods of sheetwash and calcareous precipitation on a low gradient plain. Widespread occurrence of desiccation related features within the palustrine limestones of the Jabalpur sub-region suggests that fluctuations in water levels were common, and that the topographic lows on the alluvial plain were also exposed frequently.

Episodes of sediment movement involving bedrock materials (chert, jasper, vein quartz, schist) and reworking of alluvial plain sediment (mud and calcrete clasts) affected the plain. Although desiccation and calcrete formation involves a period of moisture deficit, no evaporitic intercalations are observed. Also, in a semi-arid setting, palustrine limestones, because of periodic high alkalinity, lack evidence for extensive vegetation cover (Platt and Wright, 1992) which possibly explains the absence of biogenically-dominated calcrete fabrics.

A marine peritidal to tidal environment of deposition has been advocated for the Lower Limestone (Chanda, 1967; Singh, 1981). However, Brookfield and Sahni (1987) commented upon the misidentification of marine indicators such as algal structures (Chanda, 1967) and crab burrows (Singh, 1981). Although a few meniscate burrow-fills are recognised, the intense bioturbation shown by Singh (1981) in facies logs is probably the

result of non-recognition of widespread shrinkage features.

8.6. Mottled Nodular Beds

This unit consists of red, silty and clayey, very fine grained sandstone (Fig. 10), sandy marl and calcrete. Abundant carbonate pipes and tubular structures occur in several outcrops. Other prominent features include rhizocretions, green mottles, pebbles, and siliceous tubular and laminar structures (Fig. 10). Simple mottles are isolated and small, while compound mottles are larger and irregular resulting from the coalescence of smaller mottles. The mottles generally form around siliceous tubular and laminar structures.

In a particularly well developed section of the Mottled Nodular Beds at Sivni on the southern banks of the Narmada River, eleven superposed calcrete profiles occur. The three calcrete facies (Fig. 11) recognised in these profiles are:

(1) *Chalky*: weakly calcareous, powdery nodules and diffuse calcareous patches in red siltstone, distinctly mottled and with well developed siliceous tubular and laminar structures;

(2) *Nodular*: prominent calcareous nodules composed of micrite and abundant arenaceous detritus. Nodules are strongly calcareous, measure a few millimetres to a few centimetres across and are coalescing. Coalescence of nodules results in masses of carbonate within the distinctly green mottled red siltstone;

(3) *Platy*: calcrete facies consist of a strongly calcareous, highly mottled, indurated horizon with extensive development of calcic nodules with internal sediment and patchily distributed relict host sediment. Vertically elongate calcareous nodules may pass into a lower platy–nodular zone. Mud filled pedotubules, straight or curved, vertically to subvertically disposed, occur in some profiles.

Intergradations between these calcrete facies are common, for example, nodular-chalky and nodular-platy type (Fig. 11). An up profile increase in calcareous content from ~20 to 60% is observed (Fig. 12).

Fig. 10. Outcrop photograph (vertical face) of fine grained red sandstone of the Mottled Nodular Beds. Note the well developed green mottles, which commonly envelop tubular and thready siliceous structures.

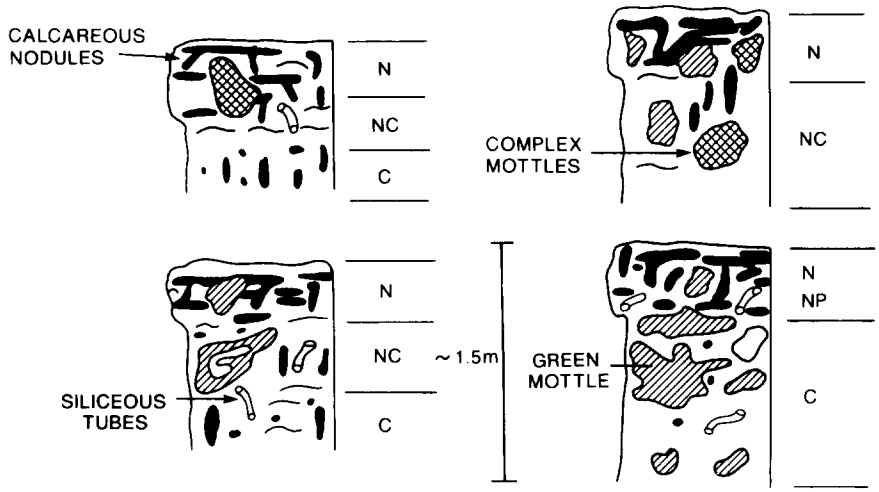

Fig. 11. Examples of calcrete profiles in the Mottled Nodular Beds at Sivni showing the vertical distribution of calcareous nodules, calcareous cement, mottles and siliceous tubular structures. *C*= chalky, *N*= nodular, *NC*= nodular-chalky, *NP*= nodular-platy.

Fig. 12. Calcrete profile (Mottled Nodular Beds at Sivni) with an upward increase in the abundance of calcareous nodules. Lower part of the profile shows localisation of the carbonate in horizontal and vertical cracks; upper part shows dense calcareous accumulation capping the profile.

In other places, well-developed calcrete profiles are less common. The mottled nodular beds, in these places, consist of mottled green, red and brown calcareous siltstone with abundant development of calcareous and siliceous nodules. Associated marl layers, though prominent, are only a few centimetres thick, laterally impersistent and may contain bivalves and ferruginous pisoids. A sauropod nesting site was recorded from a sandy, nodular and mottled calcrete. Also, some dark carbonaceous streaks in the upper part of the Mottled Nodular Beds, have yielded pollen (Dogra et al., 1988).

8.7. Petrography of Mottled Nodular Beds calcretes

The groundmass (plasma) is composed of calcite, iron oxides and clay. The most common framework grains are fine sand/coarse silt sized siliciclastic grains. Texturally, floating skeletal grains occur in micrite—the calciasepic plasmic fabric of Brewer (1976). Reprecipitation of soluble calcium carbonate has resulted in the occurrence of grain, channel and plane calcitans. Ferrans are also present. The presence of eccentric microspar coatings with a thickening downwards morphology suggests that crystal growth was, locally, affected by gravity.

Glaebules are common and occur as micrite concentrations. These are distinguishable from the enclosing plasma because of the differences in the quantity of "included" grains. Crystallaria in these calcareous palaeosols occur as tubes, chambers, and circumgranular crack fills (Fig. 13). Spar-filled cracks may merge with circumgranular crack fills.

Rhizocretion cross-sections reveal the following concentric features:

(1) core of clotted micrite followed by a microspar zone, and an external zone of carbonate with abundant floating skeletal grains;

(2) micrite core with floating skeletal grains and bifurcating microspar filled channels enveloped by a concentric zone of spar with patchily distributed micrite;

(3) core of equigranular microcrystalline quartz followed by concentric bands of spar, microspar and an outer calcareous zone with abundant skeletal grains.

The calcareous rhizocretions cement the medium-grained quartz sands. A very common texture in these is the development of isopachous rim cements of spar on the quartz grains (Mount and Cohen, 1984)

8.8. Interpretation

The well developed section of the Mottled Nodular Beds at Sivni consists of a series of vertically juxtaposed calcrete profiles developed in mottled, poorly sorted, very fine grained sandstones. There is considerable variation in lithology elsewhere. The Sivni section thus forms only a part of the interpretation, being a special element in the palaeogeomorphic and soil-catenal spectrum. The most common element is ~ 1 m thick chalky, nodular-chalky and nodular calcrete. Mottling and siliceous tubular structures are essential characteristics of the lower part of the profile. The fabrics described above suggest that these are α-calcretes (Wright, 1989). For the development of each profile, a phase of sediment accumulation, probably by sheet flooding, was followed by a period of pedogenesis, in which shrinkage caused the development of vertical fabric/vertically elongated nodules. Periods of desiccation and consequent moisture deficit are inferred, but prolonged and marked dry seasonality required for vertisol formation was absent (Ahmad, 1983). The presence of persistent green mottles and siliceous tubular structures (root casts?) is consistent with this interpretation. Repeated wetting and drying accompanied by shrinkage and growth of carbonate concretions mainly by replacement, shrinkage displacement, solution and void filling took place. The nodular horizon—the uppermost unit of the calcrete profile—is succeeded by pedogenically modified red, very fine sand, signalling an influx of clastic sediment and burial of the calcrete. Vertical variations in the character of the calcrete profiles may have resulted from several factors including variations in rates of vertical accretion (Leeder, 1975), topography and related moisture balance.

The eleven vertically juxtaposed calcrete profiles at Sivni represent sheetflood deposits succeeded by periods of calcareous pedogenesis. The degree of pedogenic modification and consequent calcrete

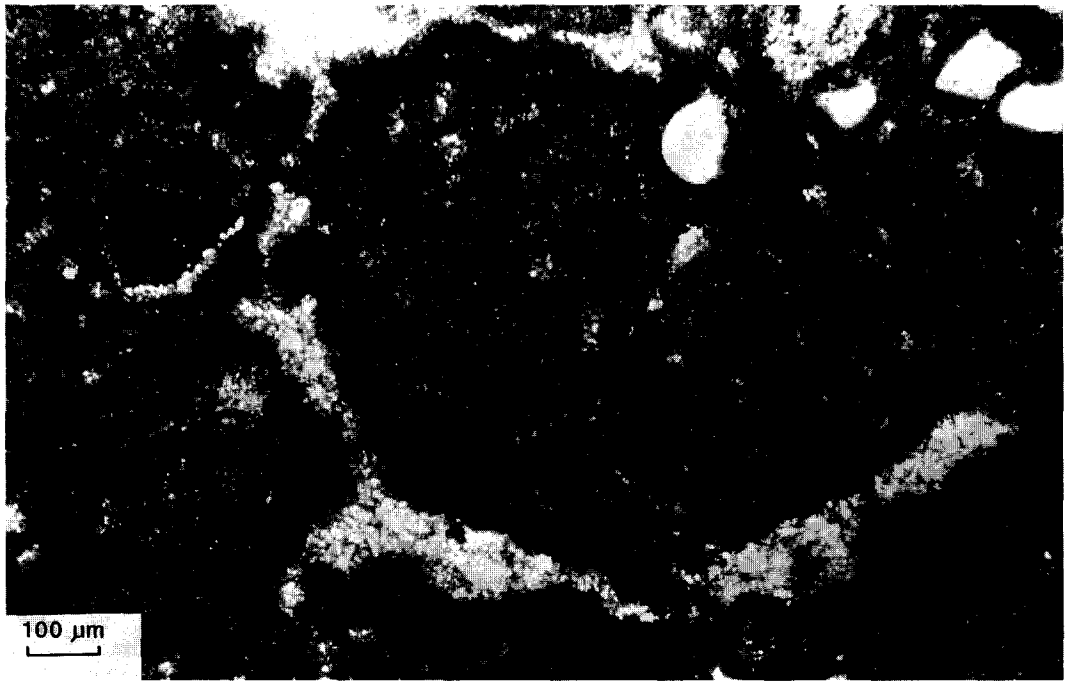

Fig. 13. Photomicrograph of micrite glaebule, circumgranular crack and spar fill in a calcrete nodule of the Mottled Nodular Beds at Lametaghat.

development is variable elsewhere. For example, although red muddy sandstone with abundant pedogenic carbonate nodules and persistent green mottles are well developed at Chui Hill, the association of a bivalve-bearing thin marl and green sandy marl, reflect poorly drained parts of the alluvial plain.

In summary, the Mottled Nodular Beds are interpreted as pedogenically modified sheetwash deposits of a semi-arid alluvial plain. Previously, these deposits were interpreted to have formed under supratidal conditions (Singh, 1981).

8.9. Upper Calcified Sandstone

This unit consists of moderately sorted trough cross-bedded sandstones which are variably calcified. For instance, at Chui Hill and Bara Simla, the sandstones are strongly calcareous and totally indurated. Within a single outcrop, calcification may be patchy, and adjacent outcrop areas vary from friable to semi-indurated to indurated. In the Jabalpur cantonment (Chui Hill, Bara Simla), the sandstones do not show any stratification.

The sandstones are quartzose and in places pebbly (jasper, chert, re-worked siliceous tubular bodies from the underlying Mottled Nodular Beds). Green mudstone clasts are locally abundant, for example at Burgi Canal and Silondi. Mudstone clasts occur in some groups of medium-scale (30–50 cm) trough cross-beds, indicating changes in flow conditions and the break up of thin mud layers into clasts.

In contrast to the palaeoflow data obtained from the basal Green Sandstone of the Lameta Beds, cross bed azimuths dip to the NE with high consistency ratios ($L = >90\%$). Calcrete petrographic fabrics include clotted micrite, linear and circumgranular spar crack fills, tangential microspar crystals growing around skeletal grains, evidence for replacive habit of calcrete, and clay skins on framework grains.

8.10. Interpretation

The widespread occurrence of this unit with a more or less uniform thickness (<5 m), in the Jabalpur region suggests deposition from widely occurring sheetfloods. The association of medium-scale trough cross-bedded sandstones, pebbly sandstones, the occurrence of locally derived detritus of green mud clasts and silica tubules, the uniformity in palaeoflow directions, and the low outcrop level variance of directional data indicate deposition from north-east directed mainly unchanneled sheetflows/sheetfloods. These deposits immediately underlie the local basal lava flow at all localities in the Jabalpur sub-region and, consequently, their calcification had been ascribed to percolating waters from the overlying traps (Chanda, 1967). This explanation is unsatisfactory as it does not explain the lack of calcification of the sandstones at Silondi or Burgi Canal in spite of their intimate association with the overlying lava flow. Although some of the calcareous accumulation may be attributed to percolating waters from overlying lava flows, most was the result of subaerial exposure and calcification in the pedogenic-vadose zone (Chui, Bara Simla). Where such calcification is absent or minimal, the Upper Sandstone is inferred to have been rapidly covered by a lava flow (for example Silondi), thereby escaping pedogenic modification, calcification and resultant induration.

9. Carbon and oxygen isotopic composition of calcretes and related facies

9.1. Methods

Subsamples of various calcareous phases were drilled from slabbed hand specimens using a microdrill and a binocular microscope. Volatile organic matter was removed by low temperature (<80°C) oxygen plasma ashing for 3 hours at 300 W forward power in a Bio-Rad PT 7300 plasma barrel etcher. Stable isotope analyses were carried out on CO_2 derived from 2 to 10 mg samples which were reacted with anhydrous H_3PO_4 at 25°C overnight. Isotope ratios were measured with a VG SIRA Series II Mass Spectrometer at the School of Environmental Sciences, University of East Anglia. Results are expressed relative to the PDB standard after correction for ^{17}O following the method of Craig (1957). The machine was calibrated using the NBS 19 and NBS 18 standards. Replicate analyses of the laboratory standard ($n = 20$) gave a 2σ precision of ± 0.04‰ for carbon and ± 0.06‰ for oxygen.

9.2. Results and discussion

Carbon isotope compositions (Table 4) for the Bagh Beds are between +0.7 and +2.0‰ ($n = 3$) and compare well with values for other Mesozoic marine limestones (e.g. Hudson, 1977; Keith and Weber, 1964). The oxygen isotope compositions for these samples are around −6‰, suggesting cementation by meteoric water, and one value is very negative (−20.6‰) suggesting thermal alteration. The carbon isotope values contrast very strongly with data from the Lameta and intertrappean beds, which generally have $\delta^{13}C$ values less than −5‰, and in many cases, less than −9‰.

The variable isotopic values in the Lower Limestone calcrete and palustrine limestones (Table 4) are plotted on Fig. 14. The palustrine limestone data have $\delta^{18}O$ values between −4.5 to −7‰. The calcrete values have generally similar carbon isotope compositions, but lighter $\delta^{18}O$ values (generally around −8 to −9‰). Freshwater and pedogenic carbonate is often dominated by CO_2 derived from the decay of plant material. Carbonaceous material at the base of the Lameta Beds has a $\delta^{13}C$ of −22‰ (Table 5), indicative of "C3" type plant metabolism (see below). Due to fractionation in the CO_2–HCO_3–$CaCO_3$ system, decaying "C3" organic matter is unlikely to produce soil-zone or lacustrine carbonate with $\delta^{13}C$ values lighter than −12 to −13‰ (see Cerling 1984; Burns and Rossinsky 1989) and calcretes of all ages have a mean $\delta^{13}C$ around −4‰ (Talma and Netterberg, 1983). Clearly the Lower Limestone data demonstrate a strong input of soil-zone carbon.

The oxygen isotope composition of pedogenic carbonate is determined by the isotopic composition of the water (rainfall), water temperature,

Table 4
Stable isotopic composition of Late Cretaceous calcareous lithofacies of the Narmada Valley

Sample no.	Locality	Stratigraphic/facies data	$\delta^{13}C$ (‰)	$\delta^{18}O$ (‰)	Remarks
Intertrappean Beds $n=6$					
1	Lametaghat (SB)(J)	Intertrappean lst	−10.43	−12.55	Basalt flow
2	Lametaghat (SB)(J)	Intertrappean lst–dark	−9.40	−8.18	at Lametaghat
3	Bharela (J)	Intertrappean beds–bivalve shells in mudstone	−10.08	−7.46	Mudstone, Limestone and tuff
4	Bharela (J)	Intertrappean beds–compact buff lst	−10.17	−10.68	
5	Bharela (J)	Intertrappean beds–compact buff lst	−10.72	−10.30	
6	Bharela (J)	Intertrappean Beds–compact buff lst	−10.66	−10.27	
Upper (calcified) Sandstone $n=1$					
7	Bara Simla (J)	Sandy calcrete	−10.25	−6.94	
Mottled Nodular Beds $n=17$					
8	Lametaghat (NB)(J)	Rhizocretion	−10.94	−8.81	
8A	Lametaghat (NB)(J)	Cemented sandstone with rhizocretions	−10.14	−8.80	
9A	Lametaghat (SB)(J)	Sauropod calcareous eggshell	−13.14	−5.31	
9B	Lametaghat (SB)(J)	Sandy brecciated nodular calcrete	−10.78	−9.95	Eggshell bearing calcrete
9C	Lametaghat (SB)(J)	Sandy brecciated nodular calcrete	−10.80	−9.12	
10	Bara Simla (J)	Pisoidal calcrete	−10.11	−8.78	Calc. pisoids and ferruginous
11A	Lametaghat (NB)(J)	Micrite-rhizocretion (zoned)	−5.10	−5.44	Internal part
11B	Lametaghat (NB)(J)	Micrite-rhizocretion (zoned)	−3.97	−4.22	External part
12A	Chui Hill (J)	Green marl	−10.15	−8.33	
12B	Chui Hill (J)	Red marl	−10.52	−8.33	
13	Lametaghat (NB)(J)	Vertically elongate calc. nodule	−10.61	−8.51	
14	Chui Hill (J)	Pedotubule in red calc. palaeosol	−9.83	−9.06	
15	Lametaghat (NB)(J)	Calc. rhizocretion	−9.85	−8.44	
16	Amkoh (J)	Calc. rhizocretion	−11.90	−6.69	
17	Amkoh (J)	Calc. rhizocretion	−12.04	−6.76	
18A	Bara Simla (J)	Pedotubule	−10.03	−6.83	
18B	Bara Simla (J)	Pedotubule	−10.18	−7.54	
Lower limestone $n=21$					
19	Bara Simla (J)	Green sandy/pebbly marl	−9.40	−8.18	Locally developed contains sauropod skeletons
20	Bara Simla (J)	Sandy marl	−11.19	−14.65	
21	Bara Simla (J)	Green marl	−9.81	−7.64	
22	Bara Simla (J)	Green sandy marl	−6.51	−2.00	
23	Lametaghat (NB)(J)	Buff micritic limestone	−8.04	−6.43	Palustrine carbonate
24	Chui Hill (J)	Buff micritic limestone	−9.73	−12.26	Palustrine carbonate
25	Lametaghat (J)	Grey honeycomb calcrete	−10.17	−9.66	
26	Lametaghat (J)	Grey honeycomb calcrete	−9.99	−8.14	
27	Lametaghat (J)	Honeycomb calcrete	−10.71	−7.59	
28	Lametaghat (J)	Honeycomb calcrete	−9.85	−8.44	Light spar veins
29	Bara Simla (J)	Brecciated calcrete	−9.53	−9.28	
30	Bara Simla (J)	Brecciated calcrete	−9.97	−10.23	
31	Chui Hill (J)	Sandy calcrete	−9.59	−9.15	Crack fill
32	Chui Hill (J)	Sandy Calcrete	−10.11	−10.39	Crack fill
33	Pat Baba (J)	Nodular calcrete, mottled	−9.73	−8.61	Eggshell-bearing calcrete

Table 4 (*continued*)

Sample no.	Locality	Stratigraphic/facies data	$\delta^{13}C$ (‰)	$\delta^{18}O$ (‰)	Remarks
34	Pata Baba (J)	Nodular calcrete, mottled	−9.50	−8.07	Eggshell-bearing calcrete
35	Chui Hill (J)	Brecciated-pisolitic calcrete	−10.06	−7.58	
36	Chui Hill (J)	Brecciated-pisolitic calcrete	−10.25	−8.84	White spar
37	Lametaghat (NB)(J)	Sandy brecciated calcrete	−7.75	−6.98	
38	Lametaghat (NB)(J)	Brecciated calcrete	−9.01	−7.09	Reworked "older" calcrete fragment
39	Lametaghat (NB)(J)	Sandy calcrete	−7.06	−5.27	Shrinkage fill area in palustrine lst
Lower Limestone eggshell data					
40	Lametaghat (NB)(J)	Sauropod calc. eggshell	−9.65	−6.72	
41	Pat Baba (J)	Sauropod calc. eggshell	−12.58	−3.15	cf. 33,34
42	Pat Baba (J)	Sauropod calc. eggshell	−12.43	−2.95	cf. 33,34
43	Balasinor	Sauropod calc. eggshell	−8.14	−7.36	
44	Balasinor	Host calcrete (cf. 43)	−12.51	−0.86	
45	Kukshi	Sauropod calc. eggshell	−8.98	−9.64	
46	Kukshi	Host calcrete (cf. 45)	−13.34	−2.94	
Lower Limestone-palustrine (Saugor Sub-region)					
47A	Tendukheda	Arenaceous nodular lst.	−9.40	−6.86	Palustrine
47B	Tendukheda	Arenaceous nodular lst	−9.63	−6.86	Palustrine
48A	Tendukheda	Grey nodular lst	−7.44	−4.96	Palustrine
48B	Tendukheda	Grey nodular lst	−7.99	−5.71	Palustrine
49A	Tendukheda	Brecciated lst	−7.22	−5.37	Palustrine
49B	Tendukheda	Brecciated lst	−9.59	−6.98	Palustrine
50A	Tendukheda	Brecciated lst	−8.87	−7.24	Palustrine
50B	Tendukheda	Brecciated lst	−7.63	−5.29	Palustrine
51A	Hill 423	Nodular lst	−7.36	−5.40	Palustrine
51B	Hill 423	Nodular lst	−7.47	−4.77	Palustrine
52	Hill 423	Brecciated lst	−9.57	−6.31	Palustrine
53	Hill 423	Brecciated lst	−7.73	−5.40	Palustrine
54A	Hill 423	Brecciated lst	−8.91	−5.95	Palustrine
54B	Hill 423	Brecciated lst	−8.80	−6.07	Palustrine
Green Sandstone $n = 2$					
55	Pat Baba (J)	Green sandstone, cement	−10.01	−8.67	
56	Pat Baba (J)	Green sandstone, cement	−10.20	−7.89	
Bagh Beds					
57A	Sitapuri	Nodular limestone	+1.35	−5.91	
57B	Sitapuri	Nodular limestone	+1.33	−5.92	Marine
58A	Sitapuri	Nodular limestone	+1.91	−5.31	(Turonian)
58B	Sitapuri	Nodular limestone	+1.97	−5.24	
59A	Sitapuri	Nodular limestone	+0.74	−20.67	
59B	Sitapuri	Nodular limestone	+0.78	−20.64	

J: indicates samples from the Jabalpur Sub-region, the main sampling area of this study. Sample suffixes A, B indicate sub-samples from a single hand specimen

and kinetic effects including crystallisation rate and evaporative effects. Fig. 14 shows that, in general, more positive $\delta^{18}O$ values correspond with more positive $\delta^{13}C$ values. Covariation of this kind has been linked to evaporative process (Salomons et al., 1978)—more positive values representing evaporated waters—which might explain the trend in our data. One group of palustrine values cluster

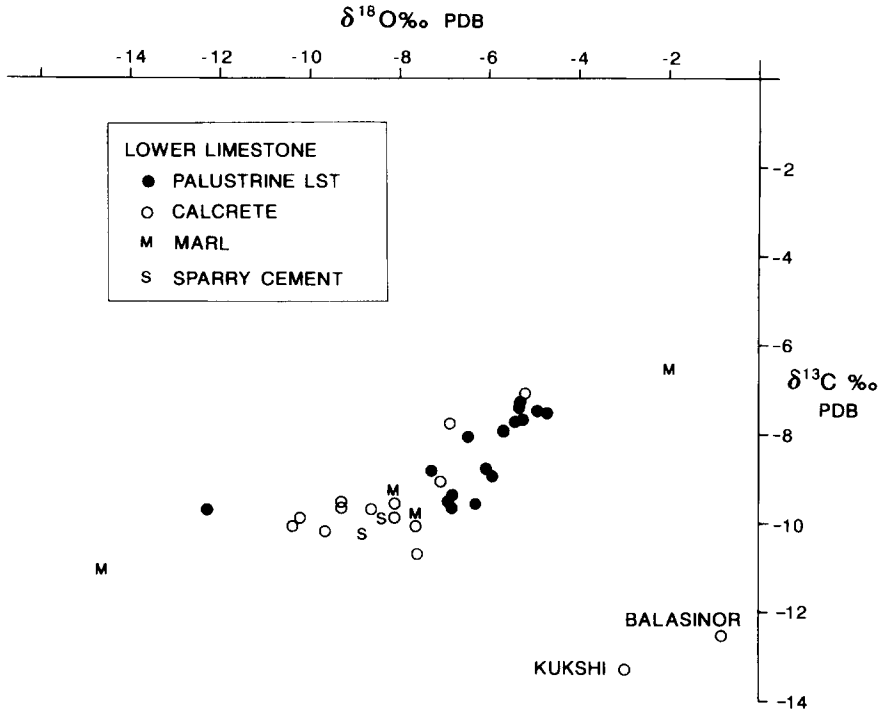

Fig. 14. Isotopic compositions of Lower Limestone calcrete and palustrine limestone. Note the lighter $\delta^{18}C$ values of calcrete and the co-variation of $\delta^{18}O$ and $\delta^{13}C$ for both subsets. Kukshi and Balasinor samples show high $\delta^{18}O$ values. (Calcrete samples—Jabalpur sub-region; Palustrine Limestone samples—mostly Saugar sub-region).

Table 5
Carbon isotope compositions of organic carbon in Lameta and Intertrappean samples. The values where wt.% organic carbon is high are probably most indicative of original $\delta^{13}C$ compositions

Sample	Locality/unit	$\delta^{13}C$ (‰)	wt.% C
LGOM-1	Lametaghat (base Lameta Beds)	−22.1	6.1
BSOM-1	Bara Simla (Mottled Nodular Beds)	−17.2	0.07
	Padwar Well (intertrappean)	−20.7	26.5

at the more positive end (−5‰) of the trend (Fig. 14), consistent with evaporation of a standing floodplain lake. If $\delta^{18}O$ values around −5‰ represent evaporated waters, then regional rainfall was presumably more negative, probably between −6 to −10‰. Two Lower Limestone calcrete samples (44 and 46, Table 4; Fig. 14) from Kukshi and Balasinor have relatively high $\delta^{18}O$ values (−1 to −3‰) indicative of evaporative processes, but retain low $\delta^{13}C$ values around −13‰.

Data for other Lameta Bed facies and intertrappean carbonates, including bivalve shells, crack filling calcrete, mottled calcrete and some crack filling cements (Fig. 15) are not generally different from the Lower Limestone values discussed above. In general the data are consistent with terrestrial–freshwater–pedogenic environments.

The exceptions are two Lower Limestone marl samples and two Mottled Nodular Beds rhizocretion samples. The oxygen isotope compositions of the marls occupy both more negative and more positive positions than the main bulk of the data (Fig. 14), suggesting evaporative effects (more positive value) and possibly thermal alteration effects (more negative value). One rhizocretion sample from Amkoh (sample 16/17, Table 4; Fig. 15) has

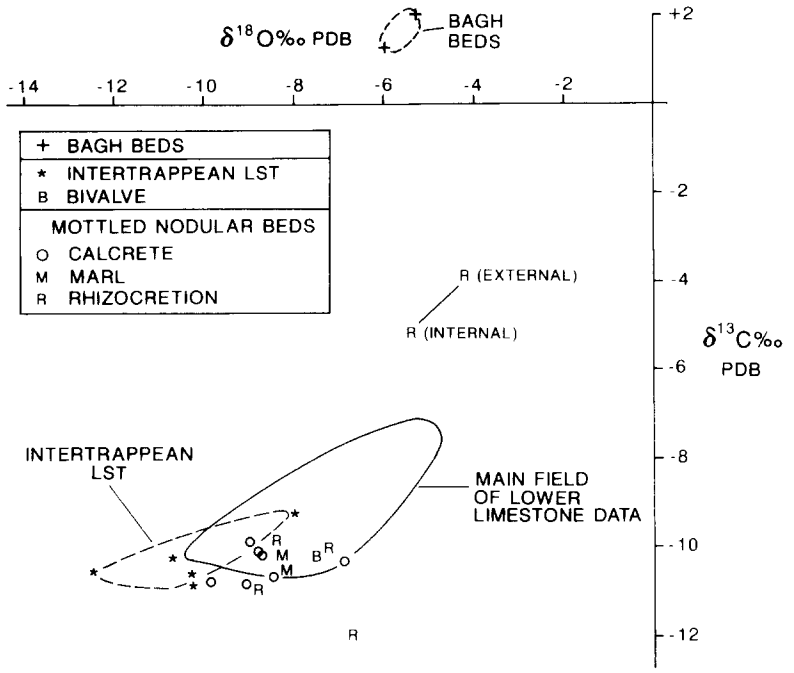

Fig. 15. Isotopic composition of the calcareous lithofacies of intertrappean and infratrappean Lameta Beds. Bulk of data centred around $\delta^{18}O$ (−8‰) and $\delta^{13}C$ (−9 to −10‰). A few rhizocretion samples show extreme values (see text for discussion).

$\delta^{13}C$ values of −12‰ which are dominated by the decay of organic matter (see above), presumably the decay of root material around which the nodule formed. Conversely, a zoned rhizocretion from Lametaghat has the heaviest $\delta^{13}C$ values of the Lameta Beds data set, −5‰ (internal zone) to −4‰ (external zone) (Fig. 15). It is not clear why this sample is anomalous, although its relatively positive $\delta^{18}O$ composition might indicate the involvement of evaporated waters from a floodplain lake in which the HCO_3^- had equilibrated with atmospheric CO_2.

There is no stratigraphic variation in isotopic compositions (Fig. 15). This suggests that palaeoenvironmental conditions, including vegetation type, mean annual rainfall isotopic composition and temperature were fairly stable during the whole depositional period of the Lameta Beds and intertrappean limestones.

Stable isotope analyses of five sauropod eggshells were made to supplement and compare with the data from the Lameta Beds of Gujarat (Sarkar et al., 1991) (Fig. 16). The eggshell isotopic values are always markedly different from—either lower or higher than—those of the host calcrete (Fig. 17). This suggests that diagenesis has not altered the eggshell values (see also Sarkar et al., 1991) and that they record valuable environmental information.

Our new data plot at the low $\delta^{18}O$ end of the Sarkar et al. (1991) data (Fig. 16). The $\delta^{18}O$ of modern reptile eggshell carbonate is almost linearly related to the $\delta^{18}O$ of water ingested by the animals (see review in Sarkar et al., 1991). By analogy, well preserved ancient eggshell material should reflect the $\delta^{18}O$ of an animal's drinking water, e.g. see Iatzoura et al. (1991). Our sauropod eggshell values vary between −3 and −10‰, suggesting that the animals drank from both evaporated water bodies (small ponds, floodplain lakes) and from water which more closely reflected the $\delta^{18}O$ of local precipitation (see above). Our eggshell $\delta^{18}O$ data did not have values as large as −2 to +8‰ (recorded by Sarkar et al., 1991). This suggests that water bodies in our study area were not extremely evaporated.

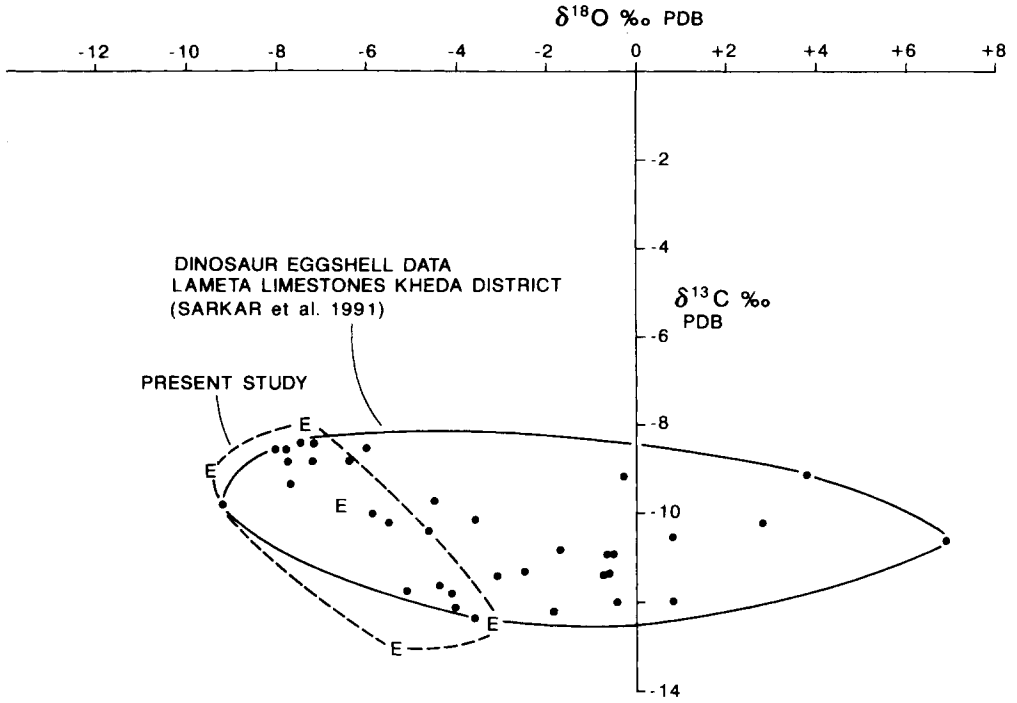

Fig. 16. Isotopic compositions of late Cretaceous dinosaur eggshell from India. Dots= data of Sarkar et al. (1991); *E*= data from present study.

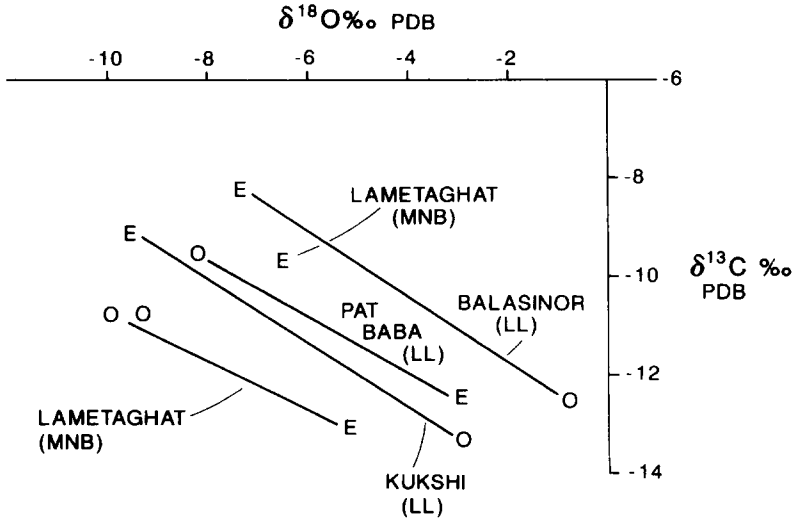

Fig. 17. Detail from Fig. 16 showing isotopic composition of eggshell calcite (*E*) and host calcretes (open circles). Note that eggshell and host calcrete are significantly different negating any diagenetic resetting of isotopic values.

The $\delta^{13}C$ of eggshell carbonate is controlled by the diet of the animal, but modified by metabolic fractionation. In modern carbohydrate feeders, eggshell carbonate seems to be about 16‰ heavier than that of the food (Von Schirnding et al., 1982; Schaffer and Swart, 1991). Our sauropod eggshell values range between −8 and −13‰. If metabolic fractionation is the only effect on $\delta^{13}C$ values in eggshells, this translates to a food source with isotopic composition in the range −24 to −29‰, values indicative of "C3" plant material. Our own analyses of $\delta^{13}C$ in carbonaceous material from the Lameta and Intertrappean Beds (Table 5) are consistent with this.

10. Discussion

The regional distribution of facies association, the petrographic character and stable isotopic composition of calcareous components, provide an integrated data set for an improved understanding of the sedimentary environments (Fig. 18) of the Lameta Beds and Maastrichtian palaeogeography of central India.

10.1. Depositional model

The basal Green Sandstone was deposited in fluvial braided channels marked by low stage conditions and ephemerality. Green detrital clays are inferred to be derived from the weathering of contemporaneous lava flows; their patchy distribution suggests across-plain tributary influences affecting the channel belt. Locally, where the Green Sandstone is thin, deposition was followed by vadose pedogenic modification.

The Lower Limestone is interpreted to represent a mixed carbonate-clastic low relief subaerial plain. Carbonate deposition took place, mostly, in desiccating ephemeral lakes/ponds. Occasional floods swept across the plain, and moved coarse sediment on to the palustrine flats. Multiplicity of facies (palustrine limestone, sheetwash detritus, and calcretes) probably occurred because of the variable influence of hydrology on different topographic elements of the plain (Platt and Wright, 1992). Changes in the hydrological system induced by shifts in weather/climate patterns significantly altered the water balance in various domains of the subaerial plain. This is clear from the association of lithofacies such as sheet sands/fissure fill diamictites (Tandon and Friend, 1989) with the palustrine limestone. In the Saugor sub-region (Fig. 1), relatively stable conditions are inferred on the plain as the Lower Limestone predominantly consists of the palustrine limestones.

The overlying Mottled Nodular Beds represent sheetwash deposits modified by periods of calcareous pedogenesis. Locally, the entire sequence of Mottled Nodular Beds may consist of multiple calcrete profiles. The predominance of red coloured sediments and associated pedogenic carbonates suggest oxidising conditions; the persistent green mottles and green marls indicate zones of moisture availability and local reducing conditions.

The Upper (calcified) Sandstone marks a period of significant sand dispersal on a north-easterly palaeoslope. Climate was wetter than before, but calcification of the sandstone in some of the sections implies that rainfall was still low at times.

The depositional and palaeopedological inferences allow the Lameta Beds to be interpreted as fluvial–palustrine–pedogenically modified sheetwash/sheets and sequences coeval with the basal Deccan lavas. Regionally, the persistent element of this sequence—the Lower Limestone—constitutes a palustrine–pedogenic surface which was buried by the thick pile of Deccan lavas. It is only fortuitous that the present depth to erosion in this eastern fringe of the Deccan province is such that this surface with its dinosaur skeletal remains and nests, is being exhumed—after 67 m.y.

10.2. Sauropod nesting site habitats

Most nesting sites occur in calcrete with evidence of repeated episodes of shrinkage, brecciation and colour mottling. The sauropod skeletal remains occur in green sandy/pebbly marls which contain ostracods, chara, and pulmonate gastropods (Sahni and Jolly, 1990). The nest-bearing Lower Limestone has both lower and upper undulatory contacts. The undulations are interpreted to be "highs" and "lows" of a subaerial surface (Mittal, 1990), and nesting sites, in some instances, can be

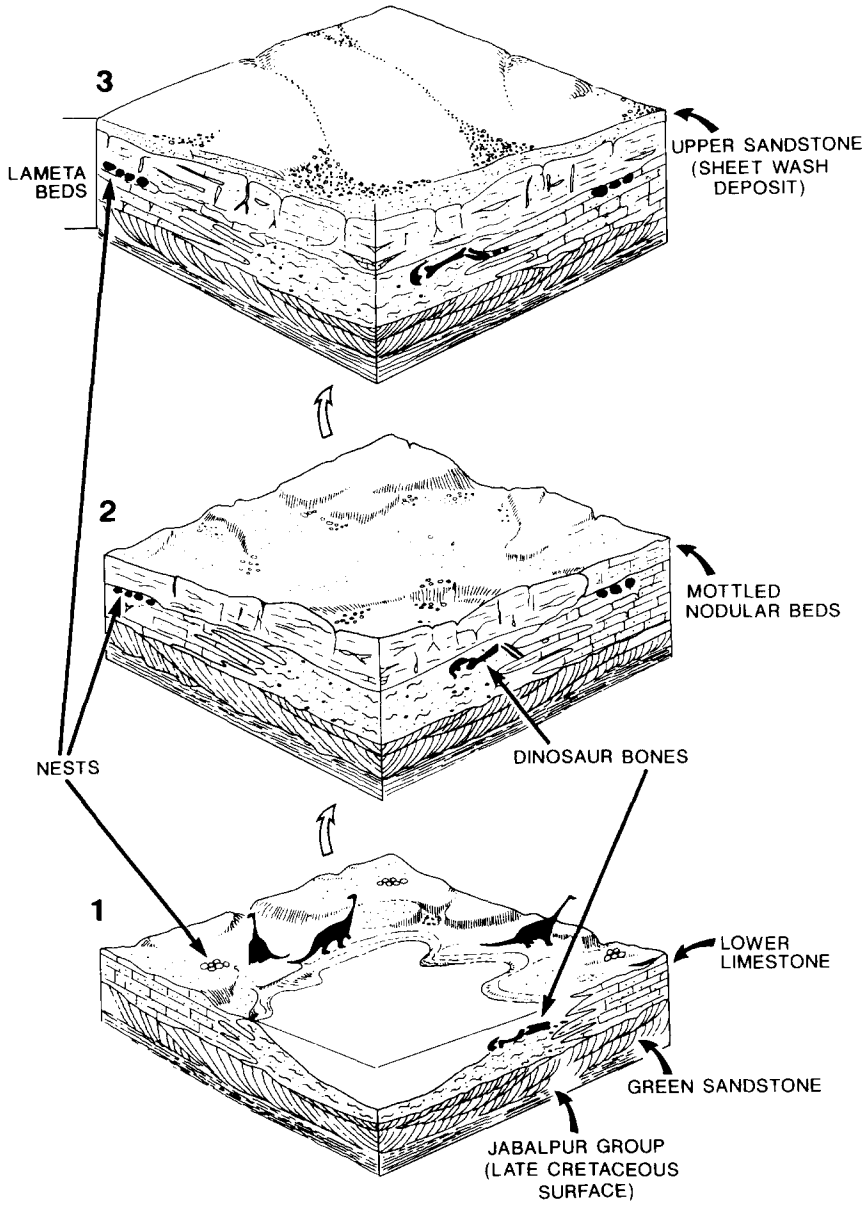

Fig. 18. Depositional model for the Lameta Beds of Jabalpur cantonment area: (1) Palustrine flat (Lower Limestone) showing lakes and emergent surfaces inhabited by sauropods. Note the palaeotopography on the flat and nesting on higher parts of the flat. (2) Burial of the palustrine–pedogenic surface by sheetwash deposits (Mottled Nodular Beds). (3) Sheetflood event representing the Upper Sandstone. Mottled Nodular Beds and Upper Sandstone are both affected by contemporaneous pedogenesis (after Sahni et al., 1994).

related to the former. Initial egg laying occurred in sheetwash detritus fringing the paludal/ephemeral lake areas. Subsequent sheetwash deposition, or lake expansion entombed the eggs in sediment. Desiccation and shrinkage events coupled with pedogenic nodule formation, cementation and

intrastratal reworking caused in situ fragmentation of eggs. In most cases, individual eggs retain their original spherical shape, but no example of a complete egg (in the stricter sense) has been found in the nesting sites of the Jabalpur sub-region. This contrasts with the spherical and nearly complete sauropod eggshells from elsewhere in the region (Mohabey, 1990; Sarkar et al., 1991).

The lack of contained embryos, hatchlings and juveniles in association with the nesting sites may be because of early entombment of the eggs in a rapidly desiccating calcium-rich host environment with abundant pedogenically induced brecciation and intrastratal reworking. Megaplant fossils are also absent from the nesting sites, although evidence of root structures (rhizocretions) are common.

10.3. Maastrichtian palaeogeography—Central India

Reconstruction of Maastrichtian palaeogeography of central India must take into consideration the sedimentary environments of the Lameta and Bagh Beds and their mutual relationship.

Our review of the environments suggests that the Late Cretaceous palaeogeographic scenario in central India was as follows:

(1) a marine incursion took place in the Turonian, in the area to the west of Indore (Bagh Beds) (Fig. 1)

(2) widespread subaerial exposure environments consisting of fluvial/palustrine/sheetwash deposits affected intermittently by pedogenesis existed in the entire Narmada region during the Maastrichtian (Lameta Beds)

(3) present-day distribution of the Bagh Beds does not indicate a widespread Late Cretaceous incursion in the upper reaches of the Narmada Valley (east of Indore); the Turonian is not represented in the Jabalpur and Saugor sub-regions indicating a period of non-deposition or erosion.

10.4. Palaeoclimate

Reconstructions of palaeolatitude for the Deccan Province place it over the Reunion Hot Spot at K–T boundary time. The Narmada region of central India is shown to have moved from about ~35°S to ~15°S during the Santonian (80 m.y.)—Palaeocene (60 m.y.) interval (Smith et al., 1981). In the reconstruction proposed by Chatterjee (1992) for the K–T boundary time, the northern limits of the Deccan province are shown at 10°S. Against this background, semi-aridity is inferred during formation of the Green Sandstone (ephemeral low stage channels), Lower Limestone (shrinkage, desiccation and brecciation) and Mottled Nodular Beds (multiple calcrete profiles). However, vertisols with shrink-swell features (concave up joints, pedogenic slickensides) are not developed, and their absence may imply a lack of well marked seasonality, with a prolonged dry season (Ahmad, 1983). Following this, wetter conditions but still with low rainfall occurred. Francis and Frakes (1993) suggested a warmer Late Cretaceous with higher CO_2 levels which have occurred because of increased CO_2 emissions from volcanic activity.

11. Conclusions

Detailed sedimentological analyses of the sauropod-bearing terrestrial deposits intimately associated with the Deccan Volcanic Province has led to the following conclusions:

(1) The Maastrichtian Lameta Beds in the Jabalpur and Saugor sub-regions of central India developed under conditions of subaerial exposure. The abundance of calcareous palaeosols in the Lower Limestone, Mottled Nodular Beds, and locally, in the Upper Sandstone indicate periods of non-deposition. The main and persistent unit of the Lameta Beds—the Lower Limestone—is an unconformity related palaeoregolith associated with the basal Deccan lavas. It was preserved by the arrival of the first lava flows. Jabalpur, the type area of the Lameta Beds, constitutes a relatively thick section (~40 m) where fluvial deposits are associated with the palaeoregolith.

(2) The Lameta Beds of the Jabalpur and Saugar sub-regions are non-marine. Late Cretaceous transgression in the Narmada Valley was limited to the region lying to the west of Indore.

(3) Stable isotope compositions of calcareous

components are consistent with a non-marine, calcrete lithofacies. Isotopically negative $\delta^{13}C$ values demonstrate a strong input of soil-zone carbon from "C3" organic matter.

(4) Lithological indicators of palaeoclimate enable recognition of semi-arid conditions with several intermittent periods of moisture deficit.

(5) Sauropod nesting mainly occurred on a palustrine–pedogenic subaerial exposure surface coeval with the initial Deccan lavas. Multiple levels of nesting sites are, in some instances, palaeotopography related. The wide geographic distribution of nesting sites in lithologically similar conditions suggest a practised sense of "site selectivity" by the Lameta sauropods.

Acknowledgements

This study was supported by the IGCP 245 National Working Group, and in particular by the Convenor, Prof. A. Sahni. The UGC SAP of the Department of Geology, University of Delhi, has provided constant support to SKT from 1990–1993. Several colleagues (Prof. V.K. Verma, Prof. V. Jhinghran) and students (R.P. Kohli, S. Kumar, Subodh Mittal, S. Chandra, V. Bose and Sandeep Mittal) have contributed to this work. Prof. V.K. Srivastava, Dr. Asit Jolly, Dr. Sunil Bajpai and Dr. S. Srinivasan are thanked for numerous fruitful discussions as well as for their excellent company during a field trip through central India in January 1992.

Stable isotopic work at the University of East Anglia was supported by an INSA-Royal Society Exchange and by funds from the School of Environmental Sciences, University of East Anglia.

The manuscript was written during a sabbatical visit of SKT to the Department of Earth Sciences, Dalhousie University, Halifax. The academic support of Dr. M.R. Gibling (Dalhousie University) and the financial support of the Canadian Bureau of International Education (Ottawa) is gratefully acknowledged. P. Judge (UEA), S. Davies (UEA) and C. Flack (UEA) prepared the final illustrations and typescript.

References

Ahmad, N., 1983. Vertisols. In: L.P. Wilding, M.E. Smeck and G.F. Hall (Editors), Pedogenesis and Soil Taxonomy 2. The Soil Orders. Elsevier, New York, pp. 91–123.

Allen, J.R.L., 1982. Sedimentary Structures, their Character and Physical Basis. Elsevier, Amsterdam.

Allen, J.R.L., 1983. Studies in fluviatile sedimentation: bars, bar-complexes and sandstone sheets (low-sinuosity streams) in the Brownstones (L. Devonian), Welsh Borders. Sediment. Geol., 33: 237–293.

Alexander, P.O., 1981. Age and duration of Deccan volcanism: K–Ar evidence. Mem. Geol. Soc. India, 3: 248–258.

Bajpai, S., Sahni, A., Jolly, A. and Srinivasan, S., 1990. Kachchh Intertrappean biotas: affinities and correlation. In: A. Sahni and A. Jolly (Editors), Cretaceous Event Stratigraphy and the Correlation of the Indian Non-marine Strata, Chandigarh, pp. 101–105.

Besse, J.E., Buffetaut, E., Cappetta, H., Courtillot, V., Jaeger, J.J., Montigny, R., Rana, R.S., Sahni, A., Vandamme, D. and Vianey-Liand, M., 1986. The Deccan traps, India and Cretaceous–Tertiary boundary events. In: O. Walliser (Editor), Global Bio-events. A Critical Approach. Springer, Berlin, pp. 365–370.

Bhatia, S.B. and Rana, R.S., 1984. Palaeogeographic implications of the Charophyta and Ostracoda of the Inter-trappean beds of Peninsula India. Mem. Soc. Géol. Fr., n.s. 147.

Bhatia, S.B., Prasad, S.V.R. and Rana, R.S., 1990. Deccan volcanism, a Late Cretaceous event: conclusive evidence of ostracodes. In: A. Sapni and A. Jolly (Editors), Cretaceous Event Stratigraphy and the Correlation of the Indian Non-marine Strata, Chandigarh, pp. 47–49.

Blanford, W.T., 1869. On the geology of the Tapti and lower Narbada valley and some adjoining districts. Mem. Geol. Soc. India, 6(3): 163–384.

Blodgett, R.H., 1988. Calcareous palaeosols in the Triassic Dolores formation, south-western Colorado. In: J. Reinhardt and W.R. Sigleo (Editors), Palaeosols and Weathering through Geologic Time Principles and Applications. Geol. Soc. Am. Spec. Pap., 216: 103–121.

Bose, V., 1992. Comparative Petrology of Jabalpur and Lameta Sandstones of Jabalpur. Thesis. Univ. Delhi, 48 pp. (unpublished).

Braithwaite, C.R.J., 1989. Displacive calcrete and grain breakage in sandstones. J. Sediment Petrol., 59: 258–266.

Brewer, R., 1976. Fabric and Mineral Analyses of Soils. Krieger, Huntington, NY, 482 pp.

Brookfield, M.E. and Sahni, A., 1987. Palaeoenvironments of the Lameta Beds, Late Cretaceous at Jabalpur, Madhya Pradesh, India: Soils and biotas of a semi-arid alluvial plain. Cretaceous Res., 8: 1–14.

Buczynski, C. and Chafetz, H.S., 1987. Siliclastic grain breakage and displacement due to carbonate crystal growth: an example from the Lenders Formation, Permian of North Central Texas, USA. Sedimentology, 34: 837–843.

Buffetaut, E., 1987. On the age of the dinosaur fauna from the

Lameta Formation, Upper Cretaceous of Central India. Newsl. Stratigr., 18: 1–6.

Burns, S.J. and Rossinsky, V., 1989. Late Pleistocene mixing zone dolomitisation, south-eastern Barbados, West Indies: discussion. Sedimentology, 36: 1135–1137.

Cerling, T.E., 1984. The stable isotopic composition of modern soil carbonate and its relationship to climate. Earth Planet. Sci. Lett., 71: 229–240.

Chanda, S.K., 1963a. Cementation and diagenesis of the Lameta Beds, Lametaghat, India. J. Sediment. Petrol., 33: 728–738.

Chanda, S.K., 1963b. Petrology and origin of the Lameta Sandstone, Lametaghat, Jabalpur, M.P., India. Proc. Natl. Inst. Sci. India, 29A: 578–587.

Chanda, S.K., 1967. Petrogenesis of the calcareous constituents of the Lameta group around Jabalpur, M.P., India. J. Sediment Petrol., 37: 425–437.

Chanda, S.K. and Bhattacharya, A., 1966. A re-evaluation of the stratigraphy of the Lameta-Jabalpur contact around Jabalpur, M.P. J. Geol. Soc. India, 7: 91–99.

Chatterjee, S., 1978. Indosuchus and Indosaurus, Cretaceous carnosaurs from India. J. Palaeontol., 52(3): 570–580.

Chatterjee, S., 1992. A kinematic model for the evolution of the Indian plate since the Late Jurassic. In: S. Chatterjee and N. Hotton III (Editors), New Concepts in Globe Tectonics. Tex. Tech. Univ. Press, Lubbock, 27, pp. 33–62.

Chiplonkar, G.W., Badve, R.M. and Ghare, M.A., 1977. Bagh Beds—their fauna, age and affinities: a retrospect and prospect. Biovigyanum, 3: 33–60.

Choudhury, J.R., 1963. Sedimentological notes on Jabalpur and Lameta formations. Q. J. Min. Met. Soc. India, 35: 193–199.

Colbert, E.H., 1984. Mesozoic reptiles, India and Gondwanaland. Ind. J. Earth Sci., 11(1): 25–37.

Courtillot, V., Besse, J., Vandamme, D., Montigny, R., Jaeger, J.J. and Cappeta, H., 1986. Deccan flood basalts and the Cretaceous/Tertiary boundary. Earth Planet. Sci. Lett., 80: 361–374.

Courtillot, V., Feraud, G., Maluski, H., Vandamme, D., Moreau, M.G. and Besse, J., 1988. Deccan flood basalts and the Cretaceous/Tertiary boundary. Nature, 333: 843–846.

Cowan, C.A. and James, H.P., 1992. Diastasis cracks: mechanically generated synaeresis-like cracks in Upper Cambrian shallow water oolite and ribbon carbonates. Sedimentology, 39(6): 1101–1118.

Craig, H., 1957. Isotopic standards for carbon and oxygen and correction factors for mass-spectrometric analysis of carbon dioxide. Geochim. Cosmochim. Acta, 12: 133–149.

Dogra, N.N., Singh, R.Y. and Kulshreshta, S.K., 1988. Palynological evidence on the age of Jabalpur and Lameta formations in the type area. Curr. Sci., 57: 954–956.

Donovan, R.N. and Foster, R.J., 1972. Subaqueous shrinkage cracks from the Caithness Flagstone series, Middle Devonian of north-east Scotland. J. Sediment Petrol., 42(2): 309–317.

Duncan, R.A. and Pyle, D.G., 1988. Rapid eruption of the Deccan flood basalts at the Cretaceous/Tertiary boundary. Nature, 333: 841–843.

Esteban, M. and Klappa, C.F., 1983. Subaerial exposure environment. In: P.A. Scholle, D.G. Bebout and C.H. Moore (Editors), Carbonate Depositional Environments. Am. Assoc. Pet. Geol. Mem., 33: 1–54.

Francis, J.E. and Frakes, L.A., 1993. Cretaceous climates. In: V.P. Wright (Editor), Sedimentology Review I. Blackwell, London, pp. 17–30.

Freytet, P., 1973. Petrography and palaeoenvironment of continental carbonate deposits with particular reference to Upper Cretaceous and Lower Eocene of Languedoc, southern France. Sediment. Geol., 10: 25–60.

Freytet, P. and Plaziat, J.C., 1982. Continental carbonate sedimentation and pedogenesis: Late Cretaceous and Early Tertiary of southern France. Contrib. Sedimentol. 12: 1–213.

Glennie, K.W., 1970. Desert sedimentary environments. In: Developments in Sedimentology, 14, Elsevier, Amsterdam, 222 pp.

Goldbery, R., 1982. Structural analysis of soil microrelief in palaeosol of the Lower Jurassic "Laterite Derivate Facies", Mishhor and Ardon Formations, Makhtesh Ramon, Israel. Sediment. Geol., 31: 119–140.

Hudson, J.D., 1977. Stable isotopes and limestone lithification. J. Geol. Soc. London, 133: 637–660.

Iatzoura, A., Cojan, I. and Renard, M., 1991. Géochimie des coquilles d'oeufs de dinosaures: essai de reconstitution Paléoenvironmentale, Maastrichtien; Bassin d'Aix-en-Provence, France. C.R. Acad. Sci. Paris, 312, 2: 1343–1349.

Jaeger, J.J., Courtillot, V. and Tapponnier, P., 1989. Palaeontological view of the ages of the Deccan Traps, the Cretaceous/Tertiary boundary, and the India-Asia collision. Geology, 17: 316–319.

Jaiprakash, B.C., Singh, J. and Ragu, D.S.N., 1993. Foraminiferal events across K/T boundary and age of Deccan Volcanism in Palakollu area, Krishna Godavari Basin, India. J. Geol. Soc. India, 41(2): 105–118.

Joshi, A. and Ganapathi, S., 1990. Carbonate-chert association in lacustrine environments of Lameta formation of Gujarat State, India. In: 13th Int. Sediment Congr. Abstr., p. 13.

Keith, M.L. and Weber, J.M., 1964. Carbon and oxygen isotopic composition of selected limestones and fossils. Geochim. Cosmochim. Acta, 28: 1787–1816.

Kohli, R.P., 1990. Mineralogy and genesis of Green Sandstone, Lameta Beds, Jabalpur area. Thesis. Univ. Delhi, 48 pp. (unpublished).

Kumar, S. and Tandon, K.K., 1977. A note on bioturbation in the Lameta Beds, Jabalpur area, M.P. Geophytology, 7: 135–138.

Kumar, S. and Tandon, K.K., 1978. *Thalassinoides* in mottled nodular beds, Jabalpur area, M.P. Curr. Sci., 47: 52–53.

Kumar, S. and Tandon, K.K., 1979. Trace fossils and environment of deposition of sedimentary succession of Jabalpur, M.P. J. Geol. Soc. Ind., 20: 103–106.

Leeder, M.R., 1975. Pedogenic carbonates and flood sediment accretion rates: a quantitative model for alluvial arid zone lithofacies. Geol. Mag., 112(3): 257–270.

Matley, C.A., 1921. On the stratigraphy, fossils and geological

relationships of the Lameta Beds of Jubbalpore. Rec. Geol. Surv. Ind., 53: 143–164.

Matley, C.A., 1923. The rocks near Lametaghat, Jubbalpore District. Rec. Geol. Surv. Ind., 55: 165–169.

McLean, D.M., 1985. Deccan traps, mantle degassing in the terminal Cretaceous marine extinctions. Cretaceous Res., 6: 235–239.

Medlicott, H.B., 1872. Note on the Lameta or the Infratrappean formations of central India. Rec. Geol. Surv. Ind., 5: 155–210.

Mittal, S.K., 1990. Facies analysis of Lameta Beds, Bara Simla Hill, Jabalpur. Univ. Delhi, 57 pp. (unpublished).

Mohabey, D.M., 1983. Note on the occurrence of dinosaurian fossil eggs from Infratrappean limestone in Kheda District, Gujarat. Curr. Sci., 52, p. 1194.

Mohabey, D.M., 1990. Dinosaur eggs from Lameta formation of western and central India: their occurrence and nesting behaviour. In: A. Sahni and A. Jolly (Editors), Cretaceous Event Stratigraphy and the Correlation of the Indian non-marine Strata, Chandigarh, pp. 86–89.

Mohabey, D.M. and Udhoji, S.G., 1990. Fossil occurrences and sedimentation of Lameta formation of Nand area, Maharashtra—palaeoenvironmental, palaeoecological and taphonomical implications. In: A. Sahni and A. Jolly (Editors), Cretaceous Event Stratigraphy and the Correlation of the Indian non-marine Strata, Chandigarh, pp. 75–77.

Mohabey, D.M., Udhoji, S.G. and Verma, K.K., 1993. Palaeontological and sedimentological observations on non-marine Lameta formation, Upper Cretaceous., India: their palaeoecological and palaeoenvironmental significance. Palaeogeogr. Palaeoclimatol. Palaeoecol., 105(1/2): 83–94.

Mount, J.F. and Cohen, A.S., 1984. Petrology and geochemistry of rhizoliths from Plio-Pleistocene fluvial and marginal lacustrine deposits, East Lake Turkana, Kenya. J. Sediment. Petrol., 54: 263–275.

Nagtegaal, P.J.C., 1969. Microtexture in recent and fossil caliche. Leidsch. Geol. Meded., 42: 131–142.

Officer, C.B., Hallam, A., Drake, C.L. and Devine, J.D., 1987. Late Cretaceous and paroxysmal Cretaceous/Tertiary extinctions. Nature, 326: 143–149.

Pascoe, E.H., 1964. Manual of Geology of India. Gov. India Publ., 3, pp. 485–1343.

Picard, L.D. and High, L.R., 1973. Sedimentary Structures of Ephemeral Streams (Devel. Sedimentol., 17). Elsevier, Amsterdam, 223 pp.

Platt, H.H. and Wright, V.P., 1992. Palustrine carbonates and the Florida Everglades: towards an exposure index for the frehswater environment. J. Sediment. Petrol., 62(6): 1058–1071.

Prasad, G.V.R., 1989. Vertebrate fauna from the infra- and inter-trappean beds of Andhra Pradesh: age implications. J. Geol. Soc. Ind., 34: 161–173.

Raiverman, V., 1975. Facies transition among Nimar, Bagh and Lameta Beds. Rec. Res. Geol. Delhi, pp. 123–139.

Raja Rao, C.S., Sahasrabudhe, Y.S., Deshmukh, S.S. and Raman, R., 1978. Distribution, structure and petrography of the Deccan traps, India. Rec. Geol. Surv. Ind., 43 pp.

Robinson, P.L., 1967. The Indian Gondwana formations—a review. In: Rev. IUGS 1st Symp. Gondwana Stratigr., Buenos Aires, pp. 201–268.

Roychoudhri, M.K. and Sastry, V.V., 1962. On the revised classification of the Cretaceous and the associated rocks of Man river section of Lower Narbada Valley. Rec. Geol. Surv. Ind., 91(2): 283–301.

Rust, B.R., 1978. Depositional models for braided alluvium. In: A.D. Miall (Editor), Fluvial Sedimentology. Can. Soc. Pet. Geol. Mem., 5: 605–625.

Sahni, A., 1984. Cretaceous–Palaeocene terrestrial faunas of India: lack of endemism and drifting of the Indian plate. Science, 226: 441–443.

Sahni, A., 1989. Paleoecology of the Late Cretaceous dinosaur eggshell sites from Peninsular India. In: D.D. Gillette and M.G. Lockley (Editors), Dinosaur Tracks and Traces. Cambridge Univ. Press, New York.

Sahni, A. and Bajpai, S., 1988. Cretaceous–Tertiary boundary events: the fossil vertebrate, palaeomagnetic and radiometric evidence from peninsular India. J. Geol. Soc. Ind., 32: 382–396.

Sahni, A. and Jolly, A., 1990. Cretaceous event stratigraphy and the correlation of the Indian non-marine strata. Chandigarh, 125 pp.

Sahni, A. and Mehrotra, D.K., 1974. Turonian terrestrial communities of India. Geophytology, 4: 102–105.

Sahni, A., Tandon, S.K., Jolly, A., Bajpai, S., Sood, A. and Srinivasan, S., 1994. Upper Cretaceous dinosaur eggs and nesting sites from the Deccan volcano-sedimentary province of peninsular India. In: K. Carpenter, K. Kirsch and J. Horner (Editors), Dinosaur Eggs and Babies. Cambridge Univ. Press, New York, pp. 204–226.

Saigal, G.C. and Walton, E.K., 1988. On the occurrence of displacive calcite in Lower Old Red Sandstone of Carnoustie, eastern Scotland. J. Sediment. Petrol., 58: 131–135.

Salomons, W., Goudie, A. and Mook, W.G., 1978. Isotopic composition of calcrete deposits from Europe and Africa and India. Earth Surf. Proc., 3: 43–57.

Sarkar, A., Bhattacharya, S.K. and Mohabey, D.M., 1991. Stable isotope analyses of dinosaur eggshells: palaeoenvironmental implications. Geology, 19: 1068–1971.

Schaffer, F.C. and Swart, P.K., 1991. Influence of diet and environmental water on the carbon and oxygen isotopic signatures of seabird eggshell carbonate. Bull. Mar. Sci., 48: 23–38.

Sharma, V., 1976. Planktonic foraminifera from Bagh Beds, M.P. In: Proc. 6th Ind. Colloq. Micropaleontol. Stratigr., Varanasi, pp. 236–244.

Singh, I.B., 1981. Palaeoenvironment and palaeogeography of the Lameta group sediments, Late Cretaceous in Jabalpur area, India. J. Paleontol. Soc. India, 26: 38–53.

Singh, I.B., Shekhar, S. and Agarwal, S.C., 1983. Palaeoenvironments and stratigraphic position of Green Sandstone, Lameta: Late Cretaceous, Jabalpur area. J. Geol. Soc. Ind., 24: 412–420.

Singh, S.K. and Srivastava, H.K., 1981. Lithostratigraphy of

Bagh Beds and its correlation with Lameta Beds. J. Paleontol. Soc. Ind., 26: 77–85.

Smith, A.G., Hurley, A.M. and Briden, J.C., 1981. Phanerozoic Palaeocontinental World Maps. Cambridge Univ. Press.

Stear, W.M., 1985. Comparison of the bedform distribution and dynamics of the modern and ancient ephemeral flood deposits in the south-western Karoo region, South Africa. Sediment. Geol., 45: 209–230.

Talma, A.S. and Netterberg, F., 1983. Stable isotope abundance in calcretes. In: R.C.L. Wilson (Editor), Residual Deposits: Surface Weathering Processes and Materials. Blackwell, Oxford, pp. 221–233.

Tandon, S.K. and Friend, P.F., 1989. Near surface shrinkage and carbonate replacement processes, Arran Cornstone Formation, Scotland. Sedimentology, 36: 1113–1126.

Tandon, S.K., Verma, V.K., Jhingran, V., Sood, A., Kumar, S., Kohli, R.P. and Mittal, S., 1990. The Lameta Beds of Jabalpur, central India: deposits of fluvial and pedogenically modified semi-arid pre-palustrine flat systems. In: A. Sahni and A. Jolly (Editors), Cretaceous Event Stratigraphyy and the Correlation of the Indian Non-marine Strata, Chandigarh, pp. 27–30.

Varma, R.K. and Banerjee, P., 1992. Nature of continental crust along the Narmada-Son Lineament inferred from gravity and deep seismic sounding data. Technophysics, 202(2–4): 375–397.

Venkatesan, T.R., Pande, K. and Gopalan, K., 1993. Did Deccan volcanism pre-date the Cretaceous/Tertiary transition? Earth Planet. Sci. Lett., 119: 181–189.

Verma, V.K., 1965. Study on the size distribution of Green Sandstone of Lameta Series from Chui Hill, Jabalpur, M.P. In: A.G. Jhingran (Editor), Dr. D.N. Wadia Commemorative Volume. Min. Metall. Inst. India, pp. 545–555.

Von Huene, H. and Matley, C.A., 1933. The Cretaceous Saurischia and Ornithischia of the central province of India. Palaeontol. Ind., 21(1): 1–74.

Von Schirnding, Y., Van Der Merwe, N.J. and Vogel, J.C., 1982. Influence of diet and age on carbon isotope ratios in ostrich eggshell. Archaeometry, 24: 3–20.

Watts, N.L., 1978. Displacive calcite: evidence from recent and ancient calcretes. Geology, 6: 699–703.

Wieder, M. and Yaalon, D.H., 1974. Effect of matrix composition on carbonate nodule crystallisation. Geoderma, 11: 95–121.

Wright, V.P., 1989. A micromorphological classification of fossil and recent calcic and petrocalcic microstructures. In: L.A. Douglas (Editor), Soil Micromorphology, Basic and Applied Science (Devel. Soil Sci., 19). Elsevier, Amsterdam, pp. 401–409.

Wright, V.P. and Tucker, M.E., 1991. Introduction. In: V.P. Wright and M.E. Tucker (Editors), Calcretes. Int. Assoc. Sedimentol., 2: 1–22.